

# **Geophex Airborne Unmanned Survey System (GAUSS)**

## **Topical Report**

**October 1993 - September 1996**

Work Performed Under Contract No.: DE-AR21-93MC30358

For

U.S. Department of Energy  
Office of Environmental Management  
Office of Technology Development  
1000 Independence Avenue  
Washington, DC 20585

U.S. Department of Energy  
Office of Fossil Energy  
Morgantown Energy Technology Center  
P.O. Box 880  
Morgantown, West Virginia 26507-0880

By  
Geophex, Ltd.  
605 Mercury Street  
Raleigh, North Carolina 27603-2343

**MASTER**

**DISTRIBUTION OF THIS DOCUMENT IS UNLIMITED** *df*

## **Disclaimer**

This report was prepared as an account of work sponsored by an agency of the United States Government. Neither the United States Government nor any agency thereof, nor any of their employees, makes any warranty, express or implied, or assumes any legal liability or responsibility for the accuracy, completeness, or usefulness of any information, apparatus, product, or process disclosed, or represents that its use would not infringe privately owned rights. Reference herein to any specific commercial product, process, or service by trade name, trademark, manufacturer, or otherwise does not necessarily constitute or imply its endorsement, recommendation, or favoring by the United States Government or any agency thereof. The views and opinions of authors expressed herein do not necessarily state or reflect those of the United States Government or any agency thereof.

## **DISCLAIMER**

**Portions of this document may be illegible electronic image products. Images are produced from the best available original document.**

## Executive Summary

This document is a Final Technical Report that describes the results of the Geophex Airborne Unmanned Survey System (GAUSS) research project. The work was performed under contract to the Department of Energy (DOE), Morgantown Energy Technology Center (contract DE-AR21-93-MC30358). The objectives were to construct a geophysical data acquisition system that uses a remotely operated unmanned aerial vehicle (UAV) and to evaluate its effectiveness for characterization of hazardous environmental sites.

Geophysical surveys of environmental sites provide a nonintrusive means of evaluating subsurface conditions. For many DOE sites, however, conditions are sufficiently hazardous that personnel cannot enter the site or must wear elaborate personal protective equipment. Rapid, digital, stand-off geophysical surveys are needed for these dangerous sites. The difficulty of developing such survey systems is compounded by the requirement that the deployed sensors must be close to the ground surface to accurately detect and characterize small targets.

The GAUSS is a data acquisition system that mitigates the potential risk to personnel during geophysical characterization of hazardous or radioactive sites. The fundamental basis of the GAUSS is as follows:

- *an unmanned survey vehicle carries geophysical sensors into a hazardous location,*
- *the pilot remains outside the hazardous site and operates the vehicle using radio control,*
- *geophysical measurements and their spatial locations are processed by an automated data-acquisition system which displays data on an off-site monitor in real-time, and*
- *the pilot uses the display to direct the survey vehicle for complete site coverage.*

The objective of our Phase I research was to develop a data acquisition and processing (DAP) subsystem and geophysical sensors suitable for UAV deployment. We integrated these two subsystems to produce an automated, hand-held geophysical surveying system. The objective of the Phase II effort was to modify the subsystems and integrate them into an airborne prototype.

The completed GAUSS DAP system consists of a UAV platform, a laser tracking and ranging subsystem, a telemetry subsystem, light-weight geophysical sensors, a base-station computer (BC), and custom-written survey control software (SCS). We have utilized off-the-shelf commercial products, where possible, to reduce cost and design time.

The GAUSS employs a remotely operated model helicopter (ROH), or other hover-craft UAV, as the survey vehicle. We selected the helicopter and hover-craft UAVs because of their inherent advantages over fixed wing and ground based vehicles. In comparison to fixed wing aircraft, the advantages of these platforms include lower air speed, superior maneuverability, and lower flight paths. Unlike ground based vehicles, these platforms can traverse difficult terrain while providing a stable sensor survey vehicle. They can traverse marsh environments, surf zones, and uneven terrain as easily as a golf course.

GAUSS uses commercial spread spectrum radio-frequency (RF) modems for telemetry between the BC and the survey vehicle sensors. We have selected radios that are capable of digital interface rates up to 19.2 kilobytes per second. These radios utilize an error correcting protocol and do not require a Federal Communications Commission (FCC) radio license.

We selected a commercial laser tracking and ranging system for use as the position measurement (POS) subsystem. The chosen instrument was designed for land surveying applications and measures distance by reflecting an infrared laser beam off an optical target attached to the survey vehicle. Servo-mechanical motors track an active LED source mounted on the rover unit and measure azimuth and depression angles. The POS subsystem provides data to the BC via a serial communications port at a rate of two position data per second.

A 100 MHz Pentium-based laptop computer is used as the BC. Custom written SCS automatically collects, processes, records, and displays data from the sensors and the POS in real-time. The software is written in C/C++ using a real-time multitasking kernel. The kernel allows multiple software tasks to run simultaneously according to their assigned priority.

We have constructed custom magnetic and electromagnetic sensors for GAUSS because suitable commercial sensors are not available. The total field magnetometer consists of a commercial three-axis fluxgate sensor, custom processing electronics, and a complimentary metal oxide semiconductor (CMOS) computer with custom-written operating software. The magnetometer electronics and sensor weigh 9.5 oz and provide total field readings at a rate of 2 samples per second with a stationary resolution greater than 1 nanoTesla (nT).

The electromagnetic induction sensor consists of a transmit and receive coil assembly, a digitally controlled transmitter, a low-noise analog receiver with analog-to-digital converter, and a digital signal-processing engine. The instrument electronics assembly occupies a single printed circuit board and is capable of multifrequency operation in the 0.3- to 18-kHz frequency band.

The magnetometer and electromagnetic sensors provide complimentary detection capabilities. The magnetometer can detect ferrous objects at extended ranges. This capability makes it useful for rapid detection and characterization of ferrous targets. The electromagnetic sensor can detect and characterize nonferrous conductive objects and environmental conditions resulting in conductivity discontinuities (i.e., meandering river beds or digging activity). Applications for the two methodologies include locating isolated objects such as drums, pipes, tanks, ordnance, and subsurface reinforced concrete structures, as well as identifying the boundaries of landfills or contaminant plumes.

We have performed numerous test surveys to evaluate the GAUSS prototype. During setup procedures, a blank map that represents the survey area is generated on the video monitor. As the sensor is moved across the site, geophysical and positional data are automatically measured, processed, displayed, and stored in real-time. At the conclusion of the survey, the data are available for post-processing and documentation.

Geophex constructed a 1/4 acre geophysical test site for evaluation of the GAUSS. The site includes buried objects placed at known depths and orientations. The test facility is designed to be realistic: nearby structures and two buried utilities contribute background noise that competes with the target anomalies.

The tests successfully demonstrated the ability of the GAUSS to simultaneously collect, process, display, and store positional and geophysical data while the survey vehicle carries a sensor in random motion.

The cost of all off-the-shelf GAUSS hardware is less than \$50,000. Because labor costs for data acquisition and processing often dominate the budget for site characterization projects, the automatic data collection and processing facilities of the GAUSS result in cost savings over traditional survey methods for operations at hazardous or radioactive sites.

## Table of Contents

|                                                                    |           |
|--------------------------------------------------------------------|-----------|
| Executive Summary.....                                             | i         |
| List of Acronyms.....                                              | v         |
| <b>1.0 Introduction .....</b>                                      | <b>1</b>  |
| 1.1 Background.....                                                | 1         |
| 1.2 Research Objectives.....                                       | 3         |
| <b>2.0 GAUSS Subsystem Development: Hardware and Software.....</b> | <b>4</b>  |
| 2.1 Data Acquisition and Processing System.....                    | 4         |
| 2.1.1 Telemetry .....                                              | 4         |
| 2.1.2 Position Measurement System.....                             | 5         |
| 2.1.3 Base Station Hardware .....                                  | 6         |
| 2.1.4 Survey Control Software.....                                 | 6         |
| 2.1.5 Sensor Platforms.....                                        | 7         |
| 2.2 Sensor Systems.....                                            | 13        |
| 2.2.1 Fluxgate Magnetometer .....                                  | 13        |
| 2.2.2 Electromagnetic Induction Instrument.....                    | 16        |
| 2.2.3 Altimeter.....                                               | 18        |
| <b>3.0 Test and Evaluation .....</b>                               | <b>20</b> |
| 3.1 Logistics.....                                                 | 20        |
| 3.2 Geophex Geophysical Test Site.....                             | 23        |
| 3.3 Demonstration Data.....                                        | 25        |
| 3.3.1 Magnetic Sensor .....                                        | 25        |
| 3.3.2 Electromagnetic Sensor.....                                  | 29        |
| <b>4.0 Discussion.....</b>                                         | <b>36</b> |
| <b>5.0 Conclusions.....</b>                                        | <b>37</b> |
| References .....                                                   | 37        |

## Figures

|              |                                                                                                                                                                                                                   |    |
|--------------|-------------------------------------------------------------------------------------------------------------------------------------------------------------------------------------------------------------------|----|
| Figure 1-1.  | Conceptual design of the Geophex Airborne Unmanned Survey System (GAUSS) for characterization of hazardous environmental sites .....                                                                              | 2  |
| Figure 1-2.  | A block diagram illustrating the major hardware subsystems of the GAUSS prototype .....                                                                                                                           | 3  |
| Figure 2-1.  | Geodimeter System 600 Instrument (left) and close-up view of the console (right) .....                                                                                                                            | 6  |
| Figure 2-2.  | Flowchart showing the fundamental logic involved with correctly assigning xyz locations to the geophysical data .....                                                                                             | 8  |
| Figure 2-3.  | BC computer screen during data acquisition. Top: Flight path and data amplitude. Bottom: interpolation option. Data acquired at the Geophex Test Facility .....                                                   | 9  |
| Figure 2-4.  | Photograph of the Schoonard X-CELL 60 series custom helicopter .....                                                                                                                                              | 10 |
| Figure 2-5.  | Photograph of Sikorsky's Cypher UAV and Geophex's EM instrument .....                                                                                                                                             | 11 |
| Figure 2-6.  | Colby CAM-COPTER .....                                                                                                                                                                                            | 12 |
| Figure 2-7.  | Photograph of Colby's Coaxial Helicopter and Geophex's EM instrument .....                                                                                                                                        | 12 |
| Figure 2-8.  | A basic block diagram of the GAUSS total field fluxgate magnetometer built by Geophex .....                                                                                                                       | 14 |
| Figure 2-9.  | [B] calculated using fluxgate data and using corrected data .....                                                                                                                                                 | 15 |
| Figure 2-10. | A simplified block diagram of the GAUSS electromagnetic sensor system .....                                                                                                                                       | 17 |
| Figure 2-11. | Block schematic of the Polaroid altimeter sensor (left). Photograph on the right shows the altimeter fastened to the Fluxgate magnetic sensor, processing circuitry, and RF modem that is used in the GAUSS ..... | 19 |
| Figure 3-1.  | Photograph of the GAUSS hardware prior to a test survey .....                                                                                                                                                     | 20 |
| Figure 3-2.  | Image of the base station screen prior starting the instruments .....                                                                                                                                             | 21 |
| Figure 3-3.  | Three reference points are necessary for establishing the transformation from the spherical coordinate system used by the Geodimeter to the rectangular system .....                                              | 21 |
| Figure 3-4.  | Image of the base station screen after the data links are established and the limits of the site are defined .....                                                                                                | 22 |
| Figure 3-5.  | Typical appearance of the graphics screen immediately after entering the graphics mode (just prior to surveying). The purpose of each window is explained in the text .....                                       | 23 |
| Figure 3-6.  | Location of buried targets within the Geophex geophysical test facility. Descriptions of the targets are provided in Figure 3-7 .....                                                                             | 24 |
| Figure 3-7.  | Description of buried targets within the Geophex geophysical test facility. See Figure 3-6 for target location .....                                                                                              | 24 |
| Figure 3-8.  | Magnetic data acquired using the pre-prototype fluxgate magnetometer .....                                                                                                                                        | 25 |



|              |                                                                                                                                                                                       |    |
|--------------|---------------------------------------------------------------------------------------------------------------------------------------------------------------------------------------|----|
| Figure 3-9.  | Photograph of the ROH and magnetic sensor package during data acquisition.....                                                                                                        | 26 |
| Figure 3-10. | Snapshot of the BC screen near the beginning of the magnetic survey using the GAUSS: left side -magnitude and location of individual data points; right side - interpolated map ..... | 27 |
| Figure 3-11. | Snapshot of the BC screen near the middle of the magnetic survey using the GAUSS: left side - magnitude and location of individual data points; right side - interpolated map .....   | 27 |
| Figure 3-12. | Snapshot of the BC screen near the end of the magnetic survey using the GAUSS: left side - magnitude and location of individual data points; right side - interpolated map .....      | 28 |
| Figure 3-13. | Topographic map produced during the magnetic survey: left side - magnitude and location of individual data points; right side - interpolated map.....                                 | 28 |
| Figure 3-14. | Magnetic data acquired using the GAUSS. The data were post processed and contoured for direct comparison to Figure 3-8 .....                                                          | 29 |
| Figure 3-15. | Electromagnetic data, 2,430 Hz in-phase component, acquired using a hand-held EM instrument with an internal data logger .....                                                        | 30 |
| Figure 3-16. | Electromagnetic data, 2,430 Hz quadrature component, acquired using a hand-held EM instrument with an internal data logger .....                                                      | 30 |
| Figure 3-17. | Electromagnetic data, 7,290 Hz in-phase component, acquired using a hand-held EM instrument with an internal data logger .....                                                        | 31 |
| Figure 3-18. | Electromagnetic data, 7,290 Hz quadrature component, acquired using a hand-held EM instrument with an internal data logger .....                                                      | 31 |
| Figure 3-19. | Real-time display of the EM data, 2,430 Hz in-phase component, acquired using a hand-held EM instrument and the GAUSS acquisition hardware and software .....                         | 32 |
| Figure 3-20. | Real-time display of the EM data, 2,430 Hz quadrature component, acquired using a hand-held EM instrument and the GAUSS acquisition hardware and software .....                       | 32 |
| Figure 3-21. | Real-time display of the EM data, 7,290 Hz in-phase component, acquired using a hand-held EM instrument and the GAUSS acquisition hardware and software .....                         | 33 |
| Figure 3-22. | Real-time display of the EM data, 7,290 Hz quadrature component, acquired using a hand-held EM instrument and the GAUSS acquisition hardware and software .....                       | 33 |
| Figure 3-23. | Post-processed EM data, 2,430 Hz in-phase component, acquired using a hand-held EM instrument and the GAUSS acquisition hardware and software.....                                    | 34 |

|              |                                                                                                                                                      |    |
|--------------|------------------------------------------------------------------------------------------------------------------------------------------------------|----|
| Figure 3-24. | Post-processed EM data, 2,430 Hz quadrature component, acquired using a hand-held EM instrument and the GAUSS acquisition hardware and software..... | 34 |
| Figure 3-25. | Post-processed EM data, 7,290 Hz in-phase component, acquired using a hand-held EM instrument and the GAUSS acquisition hardware and software.....   | 35 |
| Figure 3-26. | Post-processed EM data, 7,290 Hz quadrature component, acquired using a hand-held EM instrument and the GAUSS acquisition hardware and software..... | 35 |

### Tables

|          |                                                                     |    |
|----------|---------------------------------------------------------------------|----|
| Table 1. | Physical characteristics of the Cypher UAV.....                     | 11 |
| Table 2. | Specifications of the GAUSS Fluxgate, total-field magnetometer..... | 16 |

### Appendices

|    |                                                                              |     |
|----|------------------------------------------------------------------------------|-----|
| A. | ProxLink RF Modem Family Wireless RS-232 Connection.....                     | A-1 |
| B. | Analysis of the Novatel RT-20 GPS System.....                                | B-1 |
| C. | Schematic of the Omni-directional LED Beacon Oscillator .....                | C-1 |
| D. | New Cesium-vapor Magnetometer; the Geometrics model G-822A .....             | D-1 |
| E. | Schematics for the Fluxgate Magnetometer and Polaroid Altimeter Package..... | E-1 |
| F. | Description of the Geophex - Multifrequency Electromagnetic Sensor, GEM..... | F-1 |
| G. | Evaluation of a UAV developed by the University of Texas at Arlington.....   | G-1 |

## List of Acronyms

|        |                                                           |
|--------|-----------------------------------------------------------|
| A/D    | analog to digital                                         |
| BC     | base station computer                                     |
| BIOS   | basic input output subroutines                            |
| Bx     | reference or bucking coil                                 |
| C/A    | coarse acquisition code                                   |
| CMOS   | complimentary metal oxide semiconductor                   |
| CPU    | central processing unit                                   |
| DAP    | data acquisition and processing system                    |
| DOS    | disk operating system                                     |
| DSP    | digital signal processing                                 |
| EDM    | electronic distance measurement                           |
| EM     | electromagnetic induction                                 |
| FC     | flight computer                                           |
| GAUSS  | Geophex Airborne Unmanned Survey System                   |
| GPS    | global positioning system                                 |
| OEM    | original equipment manufacturer                           |
| OEW    | ordnance and explosive waste                              |
| ORT    | optical remote target                                     |
| PAL    | programmable array logic device                           |
| POS    | position measurement system                               |
| PWM    | pulse width modulation                                    |
| ROH    | remotely operated helicopter                              |
| RS-232 | a serial interface port standard                          |
| Rx     | receive coil                                              |
| SCS    | survey control software                                   |
| Tx     | transmit coil                                             |
| UAV    | unmanned aerial vehicle                                   |
| UART   | universal asynchronous receiver transmitter (serial port) |
| UXO    | unexploded ordnance                                       |

## 1.0 Introduction

Geophex performed the work reported in this Final Technical Report under a contract (DE-AR21-93-MC30358) from the U.S. Department of Energy, Morgantown Energy Technology Center.

### 1.1 Background

Geophysical surveys provide a nonintrusive means of evaluating subsurface conditions at environmental sites. To obtain complete characterization with currently available technologies, technicians must walk and stand at numerous locations throughout the site. These personnel may be placed at risk if hazardous material such as buried unexploded ordnance (UXO), land mines, radioactive materials, and hazardous chemicals are present. Furthermore, the cost of geophysical surveys at these hazardous sites is often increased due to safety monitoring and decontamination procedures when using conventional survey methods.

The Geophex Airborne Unmanned Survey System (GAUSS) is a data acquisition system that mitigates the potential risk to personnel during geophysical characterization of hazardous or radioactive sites. The fundamental basis of the GAUSS is:

- *an unmanned survey vehicle carries geophysical sensors into a hazardous location,*
- *the pilot remains outside the hazardous site and operates the vehicle using radio control,*
- *geophysical measurements and their spatial locations are processed by an automated data acquisition system which displays data on an off-site monitor in real-time, and*
- *the pilot uses the display to direct the survey vehicle for complete site coverage.*

Figure 1-1 depicts a GAUSS survey scenario in which a remotely controlled helicopter (ROH) carries geophysical sensors above a hazardous site. Using the GAUSS, technicians efficiently acquire geophysical data while remaining at a stand-off distance. The UAV flies at low altitude, allowing the sensors to detect weak anomalies. Geophysical data and positional data are telemetered to a BC where they are processed and graphically displayed in real-time. The display indicates the location and strength of geophysical anomalies, allowing the surveyors to modify the search or data density in real-time. The data are simultaneously recorded to a fixed disk and are available for post processing and survey documentation.

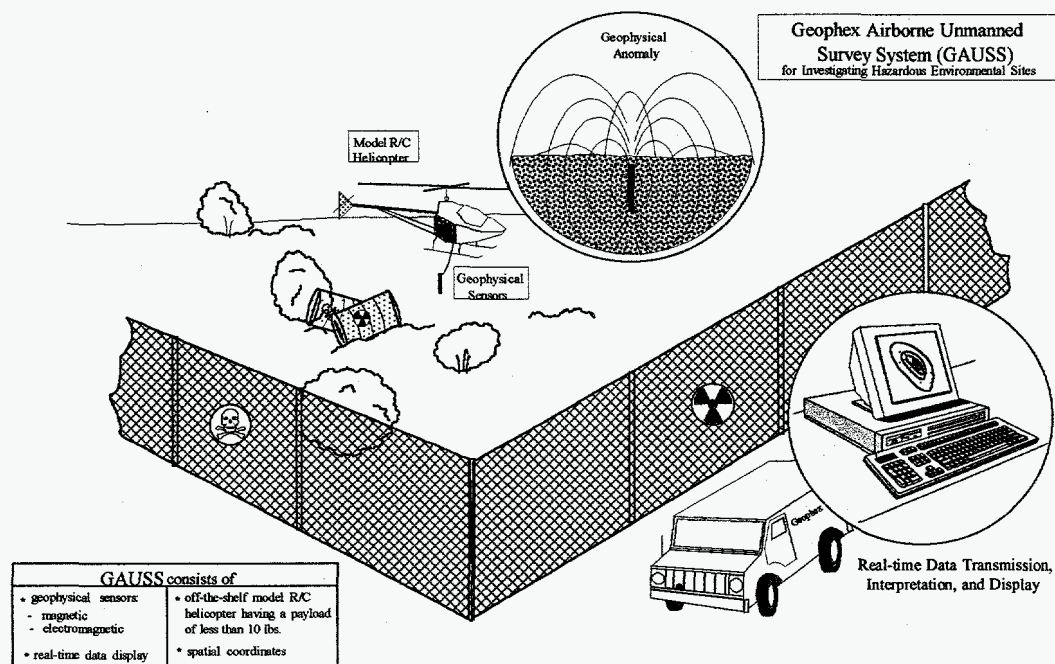


Figure 1-1. Conceptual design of the Geophex Airborne Unmanned Survey System (GAUSS) for characterization of hazardous environmental sites.

The GAUSS consists of an unmanned aerial vehicle (UAV) platform, a laser tracking and ranging subsystem, a telemetry subsystem, light-weight geophysical sensors, a base station computer (BC), and custom-written survey control software (SCS) (Figure 1-2). The GAUSS records and displays many parameters and data simultaneously. During a survey, the geophysical instruments make measurements under the control of a flight computer (FC). After processing the raw instrument data, the FC transmits the data to the BC by radio. The BC simultaneously receives unsynchronized data from the FC and from the position measurement system (POS) which tracks the UAV/sensor location.

Helicopter-based and hover-craft UAVs have no minimum air speed or minimum turning radius. These platforms, therefore, allow the sensor to be placed closer to the ground and nearer to obstacles than on fixed-wing vehicles. Unlike ground-based vehicles, the UAVs can be deployed for surveys of marshes and surf zones and can function over steep or uneven terrain while providing a stable instrument platform. No part of the GAUSS touches the site area during characterization of contaminated sites; therefore, costly and time consuming decontamination process typically required for such investigations are not required.

Section 2.0 provides information about the individual subsystems. Section 3.0 discusses the logistics of the system and presents results of experimental surveys. Sections 4.0 and 5.0 discuss the discussion and results, respectively.

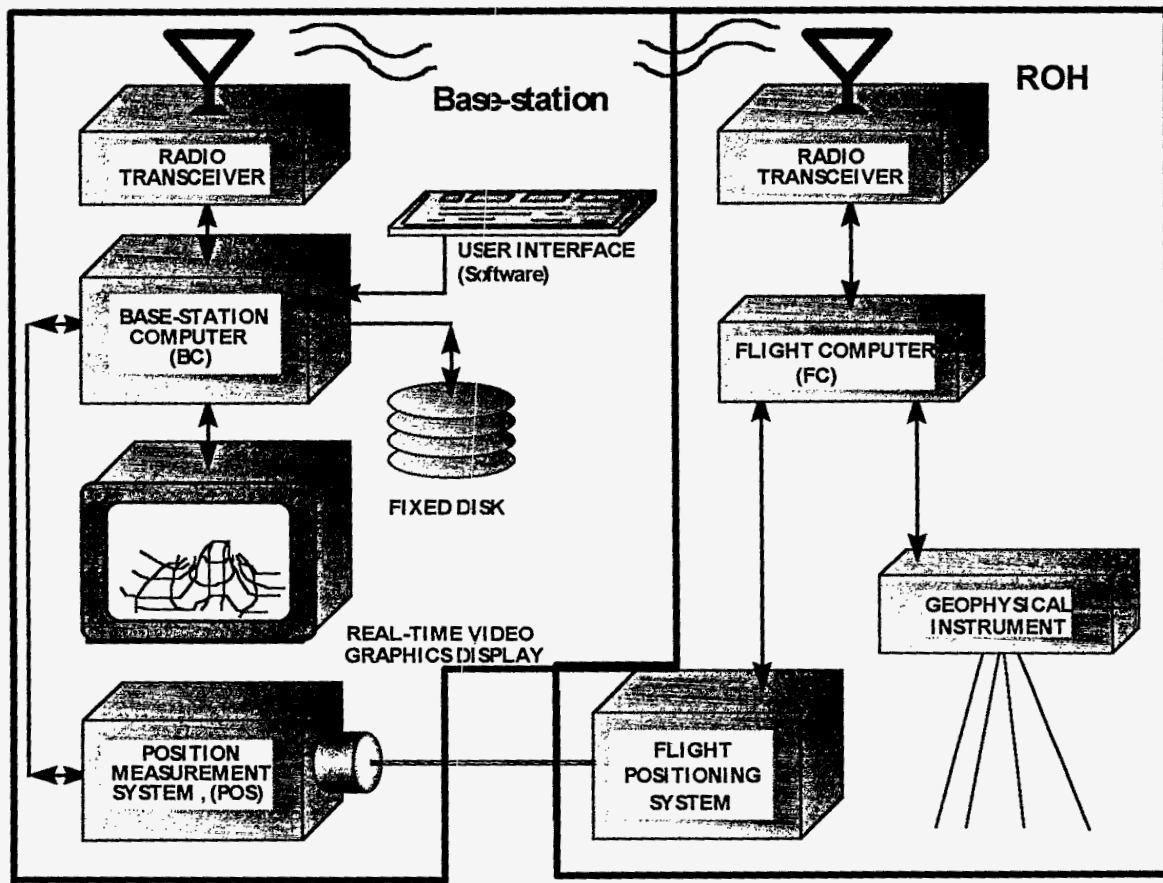


Figure 1-2. A block diagram illustrating the major hardware subsystems of the GAUSS prototype.

## 1.2 Research Objectives

This project is a feasibility study to determine the applicability of UAV-carried sensors for stand-off geophysical surveying. The ultimate objective is to apply GAUSS technology to nonintrusive surveys at DOE hazardous waste sites. The success criteria for the GAUSS include the demonstrated ability to:

1. Maneuver the sensor platform (viz., UAV or ROH) with full GAUSS instrumentation.
2. Automatically acquire position, altimeter, and sensor data.
  - a. Design, construct, and test digital geophysical sensors suitable for UAV-borne application.
  - b. Acquire a light-weight, two-way digital telemetry system and incorporate a communications protocol featuring error detection and correction capabilities.
  - c. Acquire and integrate a suitable, real-time electronic position measurement system.
  - d. Develop software algorithms for remote instruments and the base-station that perform sensor control, digital communication and error detection; provide a positioning system interface; and record, process, and display the acquired data.
3. Display the results of test surveys in real-time.

## 2.0 GAUSS Subsystem Development: Hardware and Software

The GAUSS consists of six subsystems; 1) survey platform, 2) geophysical sensor (viz., magnetometer or electromagnetic induction), 3) base-station computer and survey control software, 4) positioning system, 5) altimeter, and 6) telemetry. In this section, we discuss the details of each subsystem.

We have used commercial off-the-shelf hardware and software products, whenever possible. Use of commercial products reduces development cost, increases system reliability, improves serviceability, allows easier system upgrade, and reduces cost. Geophex constructed custom-built components only when suitable commercial products were not available.

The overall considerations guiding subsystem design and development were:

1. **Size and weight.** The maximum weight budget for the ROH payload is 8 lb.
2. **Performance.** GAUSS must be efficient, produce high quality data, and be practical to use.
3. **Durability.** The hardware must be able to withstand the rigors of daily field use. Software must be robust and able to gracefully recover from data errors.
4. **Cost.** The system must be affordable, making it a viable alternative to other methods of site characterization.

### 2.1 Data Acquisition and Processing (DAP) System

The functions performed by the DAP system are central to GAUSS operation. The objectives of the DAP system are to track the location of the survey vehicle, receive sensor and position data concurrently, and interpret, display, and store the data in real-time. The completed DAP functions are automated and do not require human intervention after system initialization. The DAP system includes the telemetry subsystem (Section 2.1.1), the position measurement subsystem (Section 2.1.2), base-station hardware (Section 2.1.3), survey control software (Section 2.1.4), and the sensor platform (Section 2.1.5).

#### 2.1.1 Telemetry

The FC communicates geophysical sensor data and status information to the BC via a digital, spread-spectrum, radio-frequency (RF) modem (Proxim model PL-2). The PL-2 features transparent error detection and correction with interface rates up to 19.2 kilobits per second. The radio digital transmission rate (viz., the transmission between modems) is 242 kilobits per second. The spread spectrum modulation technique uses the 902-928 MHz band, which allows high reliability communication with 0.5 W transmission power. The radios can be used anywhere within the United States without an FCC radio license. Additional specifications of the Proxim RF modems are in Appendix A.

### 2.1.2 Position Measurement System

The positioning system must track the survey vehicle location and relay this information to the SCS. We investigated ground-based radio and acoustic positioning systems to perform this function, but decided that the logistical complexities involved with these methods prohibit their use in the GAUSS.

After investigating the ability of the Global Positioning System (GPS) and laser methods, Geophex selected a laser tracking and ranging instrument, the Geodimeter, manufactured by Geotronics. The operational characteristics of the Geodimeter are presented below. Our experiment with a real-time differential GPS system, manufactured by Novatel Communications, is presented in Appendix B.

Phase I research was conducted using the Topcon AP-L1 optical positioning system (Phase I Topical Report). The Topcon unit is a passive tracking and ranging instrument (viz., it does not use an active source located on the rover unit for tracking purposes). Because of this attribute, the Topcon instrument could not adequately track the mobile model helicopter.

To improve the position measurements, Geophex decided to employ a laser tracking system that utilizes an active, rover-mounted source during Phase II. We selected the Geodimeter System 600 due to its enhanced tracking ability and ease of use (Figure 2-1).

The Geotronics Geodimeter System 600, hereafter referred to as the Geodimeter, is a flexible total-station measurement system that is easily tailored to different user needs. The Geodimeter determines location by tracking an optical remote target (ORT), which consists of an array of infrared light emitting diodes (LEDs), and determines distance by reflecting an infrared laser light off of retroreflecting tape or corner cubes. The Geodimeter can store the measurements into a built-in data logger or output the data via an RS-232 port. GAUSS requires that the Geodimeter is set up to automatically track and range the ORT and relay the data to the BC via the RS-232 port.

The infrared measurement beam in the Geodimeter has a width of 16 cm per 100 m (~6 inches per 300 feet) and a range capability of 0.2 m to 2500 m in normal weather conditions. It is powered by an external nickel-cadmium 12 V, 6-amp-hour battery. Because the ORT supplied with the Geodimeter is not omnidirectional, Geophex fabricated an electronic circuit and hardware that is suitable for UAV deployment (Appendix C).

A restriction imposed by optical positioning is that an unobstructed line of sight must be maintained between the instrument and the reflector (viz., the survey platform). This restriction is already in effect, however, because the pilot must maintain a clear view of the UAV to maintain control (we did not investigate autonomous flying techniques as part of this research project). If a portion of a survey site is obstructed, the instrument and the pilot can move to a new location and the survey continued.



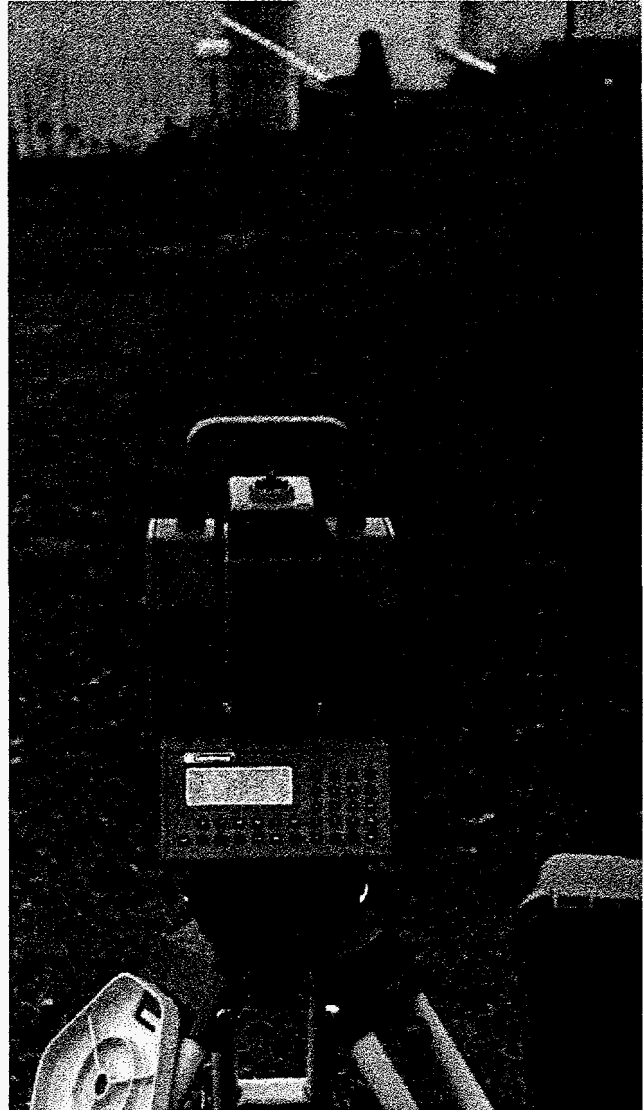
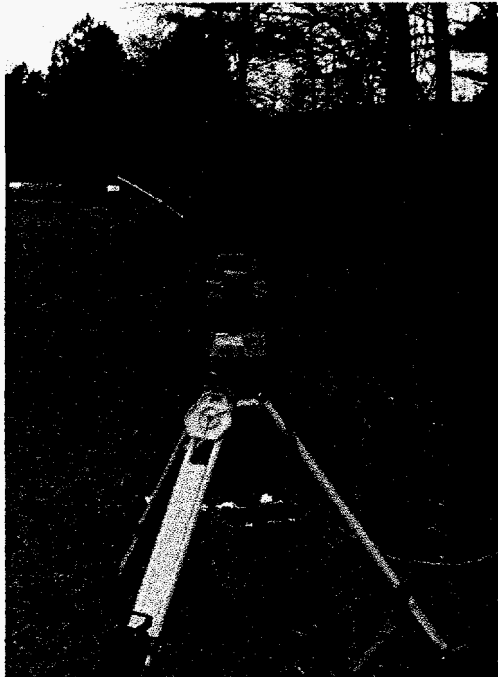


Figure 2-1. Geodimeter System 600 Instrument (left) and close-up view of the console (right).

### 2.1.3 Base Station Hardware

A 100 MHz Pentium-based laptop computer running DOS (or WIN 95 started in "command prompt only" mode) with a VGA color display is used as the GAUSS base station. Two serial ports are required to simultaneously record spatial registry and geophysical data.

### 2.1.4 Survey Control Software (SCS)

The SCS ties the GAUSS subsystems together and defines the operational characteristics of the system. The SCS is written in C/C++ and compiled using Borland 4.0. The SCS requires DOS graphics libraries that are provided by Borland 4.0. The core of the program is a commercial real-time multitasking kernel (RTKernel 4.0 from *On Time Corporation*). RTKernel establishes a

“cooperative multitasking” environment, where each task receives CPU time based on its priority and cooperative scheduling.

The SCS receives, processes, displays, and stores the position, altimetry, and geophysical data in real time. Because the BC receives data from the geophysical sensor and POS asynchronously, the first priority is to properly correlate the two data streams. This is accomplished by buffering the data streams and using time stamps (Figure 2-2). After the geophysical and spatial registry data are matched, the data pair is simultaneously displayed on the computer screen and written to hard disk.

The majority of the SCS code is devoted to processing and displaying the data in real-time. The SCS allows the user to save an image of the screen (i.e., a “snapshot” in time) during acquisition. It also allows the user to change the portion of the survey area displayed on the screen and the color scale. A very useful feature of the program is the ability to display a color map (instead of individual data points) of the survey area. All the functions can be invoked at any time without interrupting the survey and interfering with the prime tasks of collecting, time-stamping and matching, and recording the data to disk. In addition to the graphic display of the geophysical data (linked to its spatial coordinates), the BC computer screen (Figure 2-3) displays the following information:

- the CPU demand and survey date,
- the incoming data stream for the Geodimeter and geophysical sensor,
- the power supply voltages,
- the number of data points acquired,
- the number of snapshots recorded,
- the numeric value of the geophysical data (last collected),
- color scale limits,
- minimum and maximum of the displayed survey area shown on the screen,
- the number of pixels representing each data point,
- redraw capability,
- interpolation feature (viz., generates a 2-D color map), and
- a list of functions that can be invoked with “hot keys”.

### 2.1.5 Sensor Platforms

In this section, we present Geophex’s ROH and present alternative platforms that have been developed by others since the GAUSS project started in 1993.

#### 2.1.5.1 Remotely Operated Helicopter (ROH)

Geophex purchased a Schoonard X-CELL 60 series custom helicopter, manufactured by Miniature Aircraft USA, for use in the GAUSS (Figure 2-4). This helicopter model is capable of lifting a maximum payload of 15 pounds and has routinely been used by others to carry an 8-pound video camera for 25-minute sorties.

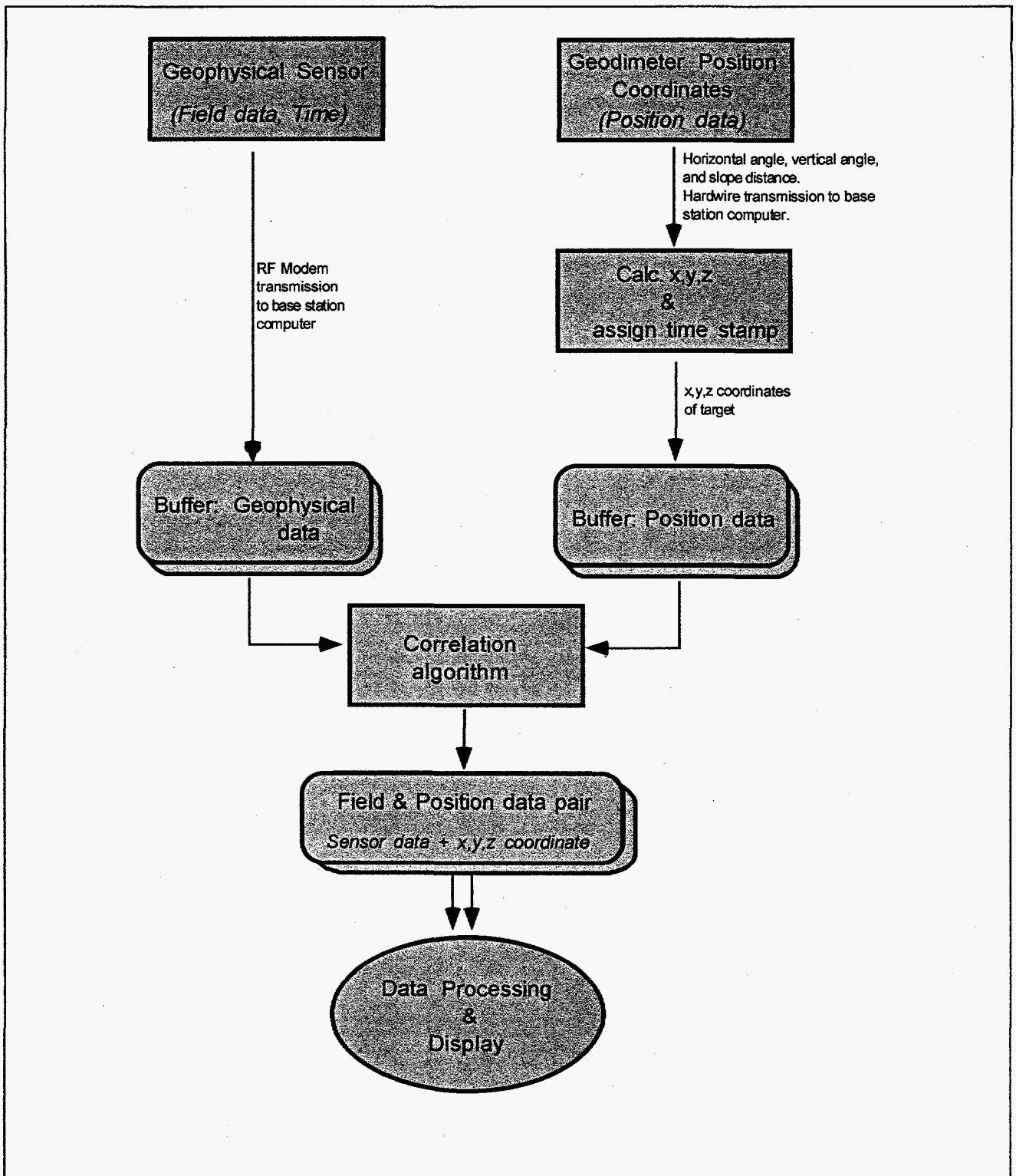


Figure 2-2. Flowchart showing the fundamental logic involved with correctly assigning xyz locations to the geophysical data.

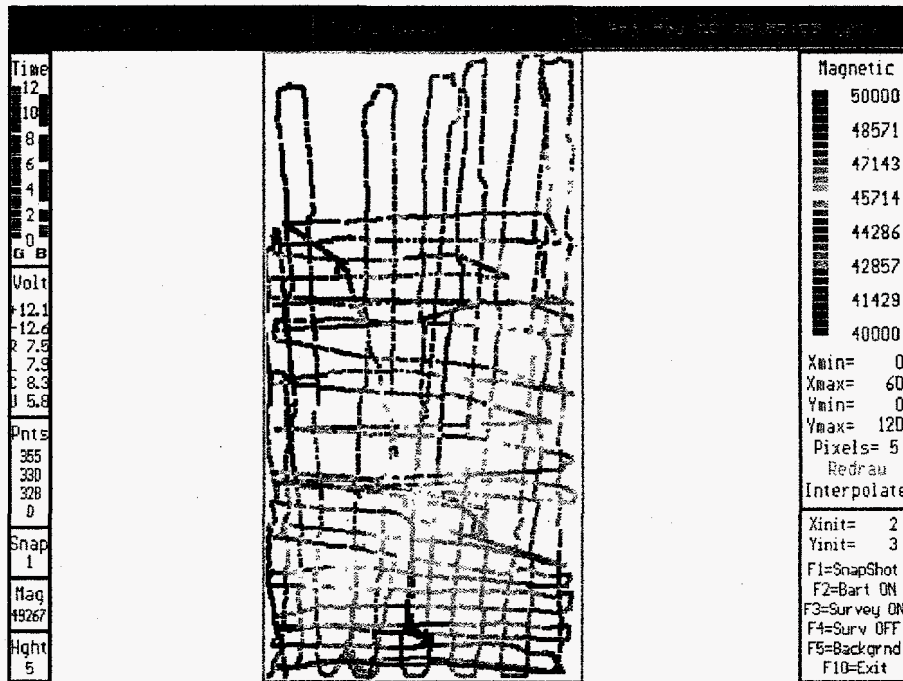


Figure 2-3. BC computer screen during data acquisition. Top: Flight path and data amplitude. Bottom: interpolation option. Data acquired at the Geophex Test Facility.



Figure 2-4. Photograph of the Schoonard X-CELL 60 series custom helicopter.

The ROH construction material is mostly aluminum and stainless steel with wooden rotor blades. Some ferrous material is used, which results in a 50 nT anomaly when detected at 2 feet by the GAUSS magnetometer. To reduce the signature from the UAV, we rigidly fixed the position of the sensors with respect to the ROH, so that the anomaly caused by the helicopter results in a constant shift in the instrument baseline readings. The target anomalies are not influenced by the constant offset due to the ROH. This technique is commonly used in sensor instrumentation construction and in full-scale airborne geophysical surveys.

The ROH does not touch the ground during the course of a survey and is capable of functioning over water and surf zones. Advantages of the ROH over ancillary hover-craft UAVs include low cost (both initial and replacement) and availability. The primary limitations of the ROH are 1) a practical payload of less than 10 pounds, 2) it must remain visible to the pilot, 3) it cannot fly in wind speeds greater than 10 miles per hour, and 4) fragility.

#### 2.1.5.2 Alternative Unmanned Airborne Vehicles

To circumvent the restrictions imposed by the ROH, we investigated alternate UAVs that have been recently developed by others. Two alternate vehicles are described below.

Sikorsky Aircraft developed an UAV, named the Cypher, for the Defense Department's now defunct unmanned aerial vehicle maneuver effort. Cypher is a 6.5-ft-diameter, doughnut-shaped UAV driven by two independent coaxial rotors that are powered by a 52-hp., 2-cycle rotary engine. The Cypher UAV began untethered flight testing in April 1993. Although the Cypher was designed to be a reconnaissance vehicle carrying cameras for surveillance and security missions, commercial applications include attaching geophysical sensors for detecting ordnance or underground facilities. The Cypher uses GPS measurements for spatial registry and is capable of waypoint flying. The Cypher characteristics are presented in Table 1.

**Table 1. Physical Characteristics of the Cypher UAV.**

|                           |                       |          |
|---------------------------|-----------------------|----------|
| <b>Overall Dimensions</b> | Fuselage Diameter     | 6.5 feet |
|                           | Fuselage Height       | 2.0 feet |
| <b>Weights</b>            | Weight Empty          | 175 lb.  |
|                           | Normal Takeoff Weight | 255 lb.  |
|                           | Maximum Gross Weight  | 300 lb.  |
|                           | Sensor Payload Weight | 45 lb.   |

Geophex participated in a joint technology demonstration project with Battelle, Pacific Northwest National Laboratories, during 1996. The objective of the demonstration was to attach magnetic and electromagnetic sensors on the Cypher UAV. The photograph in Figure 2-5 shows Geophex's electromagnetic instrument mounted on the Cypher prior to flight. Although the Cypher produces significant magnetic and electromagnetic interference, results of the tests indicated that the Cypher can be used as a geophysical survey platform.

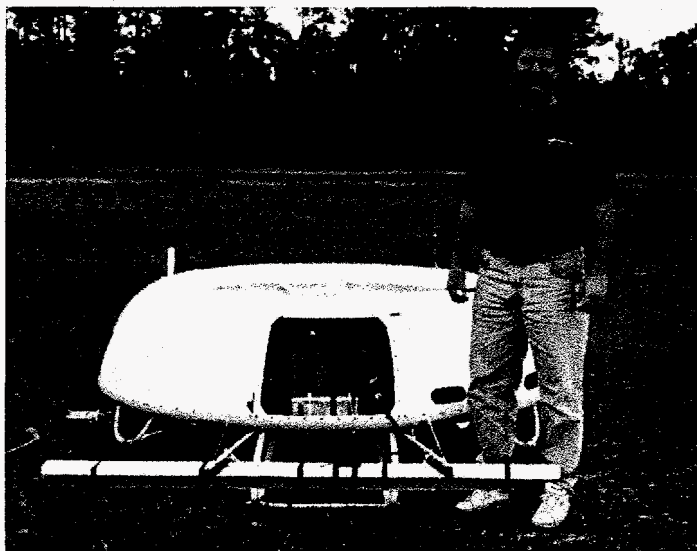


Figure 2-5. Photograph of Sikorsky's Cypher UAV and Geophex's EM instrument.

A second, lower-cost, commercial UAV is currently under development by Colby Systems from Palo Alto, CA. The Colby CAM-COPTER (Figure 2-6) has a 7.5-ft diameter rotor, a 30-pound payload capacity, and can cruise at 65 mph. This UAV is primarily used for taking aerial shots for the movie industry.

A newer version, the Colby Coaxial Helicopter with two counter-rotating main rotors, is in the final testing phase (shown in Figure 2-7 with Geophex's EM instrument). One of the salient features of Colby's new UAV is that if for any reason the remote control signal is lost, the helicopter goes into a hovering mode, staying stationary until remote control is restored. Both Colby helicopters weigh less than 35 pounds.

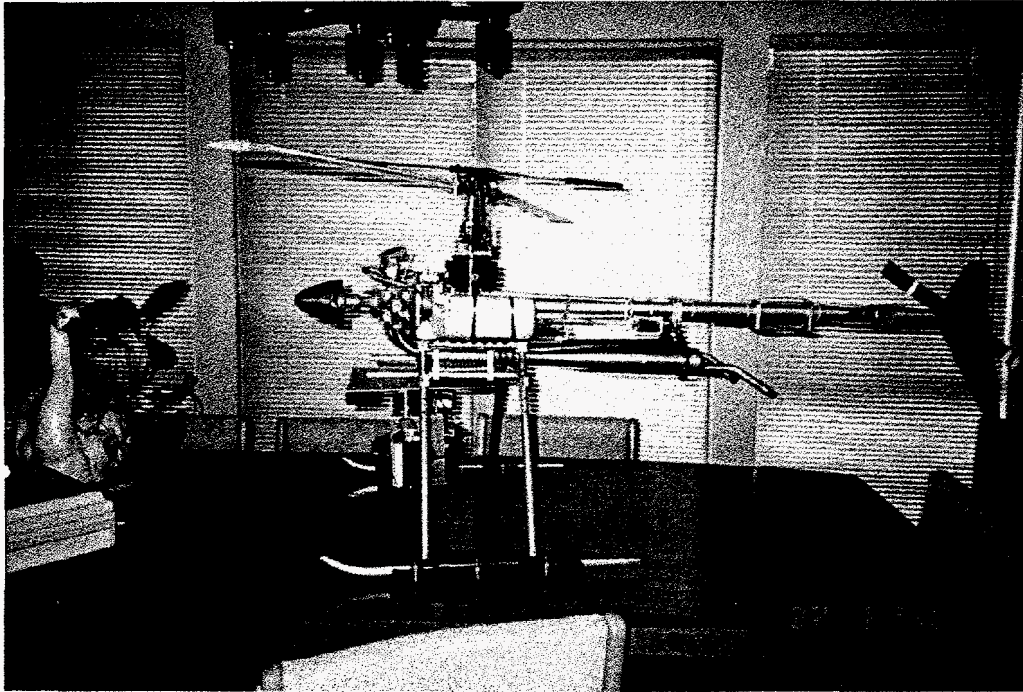


Figure 2-6. Colby CAM-COPTER.



Figure 2-7. Photograph of Colby's Coaxial Helicopter and Geophex's EM instrument.

## 2.2 Sensor Systems

The geophysical sensors employed in GAUSS include a total field magnetometer and an EM induction sensor. We have selected these methods because they are complimentary and widely applicable for environmental site characterization. Targets that can be detected using these methods include UXO, subsurface drums, pipes, and reinforced concrete structures. Ancillary uses of these techniques includes locating the edges of landfills, pits or trenches; mapping chemical leach fields; locating shallow subsurface voids or structures; shallow water marine bathymetry; and detection of conductive subsurface objects or native media.

Magnetic sensors that meet the size, weight, power consumption, and performance requirements of GAUSS did not exist commercially until Spring 1996. Consequently, Geophex designed and fabricated a custom, total-field magnetometer using a fluxgate sensor. Details of our total-field magnetometer are presented in Section 2.2.1. A scalar, cesium-vapor magnetometer that is suitable for use in GAUSS is under development by Geometrics, model G-822A. This sensor was tested by Geophex personnel during May 1996. Results of our tests are briefly presented in Appendix D.

Broadband EM induction sensors that are suitable for use in the GAUSS do not exist commercially. Under this research project, we modified and enhanced our own proprietary EM sensor. A description of our EM instrument is presented in Section 2.2.2.

### 2.2.1 Fluxgate Magnetometer

Geophex constructed a lightweight, total-field magnetometer using a commercial, three-axis fluxgate sensor, the Bartington Instruments model MAG03MCL. The functionality of the total field magnetometer is illustrated in Figure 2-8. The fluxgate sensor provides three field-voltages,  $V_x$ ,  $V_y$ ,  $V_z$ , each proportional to the component of the magnetic field aligned with the respective fluxgate axis. The field-voltages are buffered and filtered by three-channel analog circuitry. Low-pass filtering is used to remove the strong 15.625-kHz component that is caused by the fluxgate excitation oscillator.

Although the GAUSS magnetometer package employs a commercial fluxgate sensor, the signal processing and conditioning is accomplished with a PCB that was designed and built by Geophex for this project. The filtered field-voltages are sampled and digitized simultaneously by a bank of AD7703 20-bit, sigma-delta, analog to digital (A/D) converters. The A/D converters are controlled by a CMOS computer, model 5F-LCD manufactured by Onset Computer Corporation. The computer has been modified to operate with an external 4.9152 MHz clock circuit which also drives the A/D converters. Use of a common clock allows the converters to be synchronized with each other and the computer. This synchronization significantly reduces the influence of on-board electrical interference. The CMOS computer communicates with a radio transceiver using an RS-232 port. Power conditioning circuits provide isolated power for the digital circuits and analog circuits. The fluxgate sensor is powered by a separate battery pack. Schematics for the fluxgate magnetometer are presented in Appendix E.



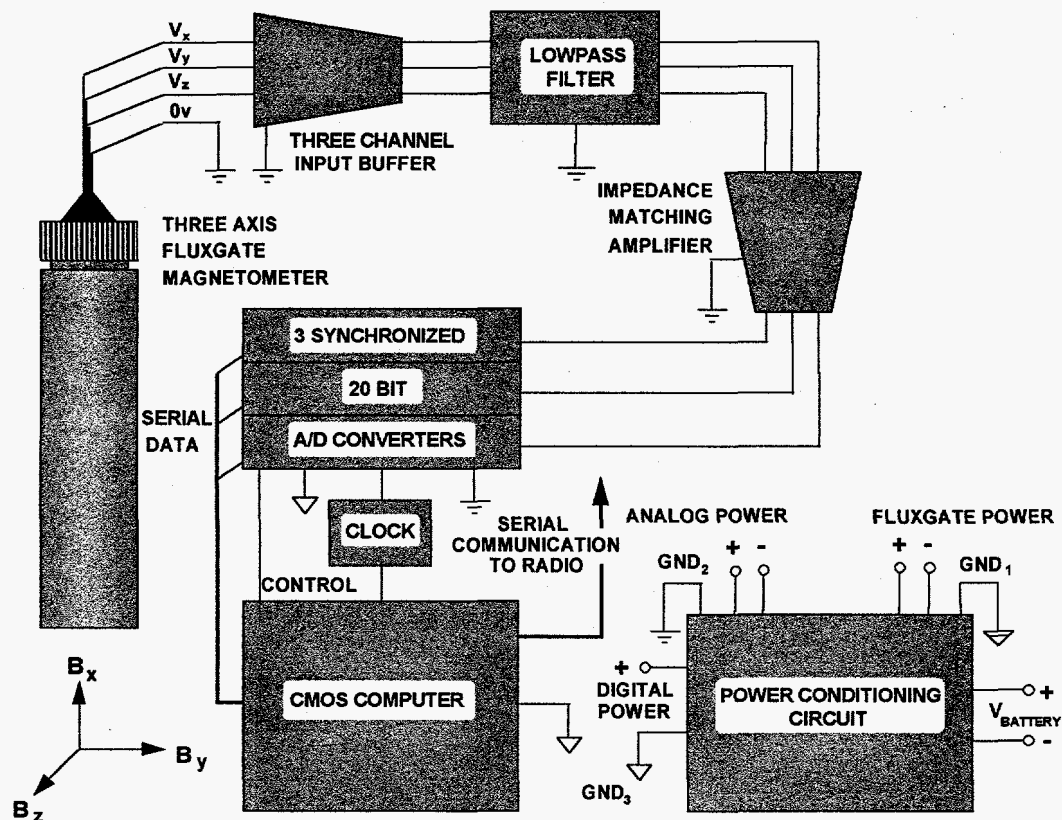


Figure 2-8. A basic block diagram of the GAUSS total field fluxgate magnetometer built by Geophex.

The computer runs a program residing in on-board non-volatile memory. The control program, which was written at Geophex, consists mainly of assembly-level drivers and interface routines to control the A/D converters. Higher level functions are performed by floating point tokenized BASIC routines. Duties of the computer include synchronization, initialization, and periodic recalibration of the A/D converters, reading and formatting of A/D data, and communication with the BC.

The BC determines field magnitude using a real-time transformation of the raw, 3-component, field data. The manufacturer guarantees fluxgate alignment to be orthogonal within  $\pm 0.5^\circ$  per axis. This slight misalignment results in considerable heading error if Pythagorean's theorem is used to calculate field magnitude using raw fluxgate data. As seen in Figure 2-9, the uncorrected heading error can exceed 240 nT.

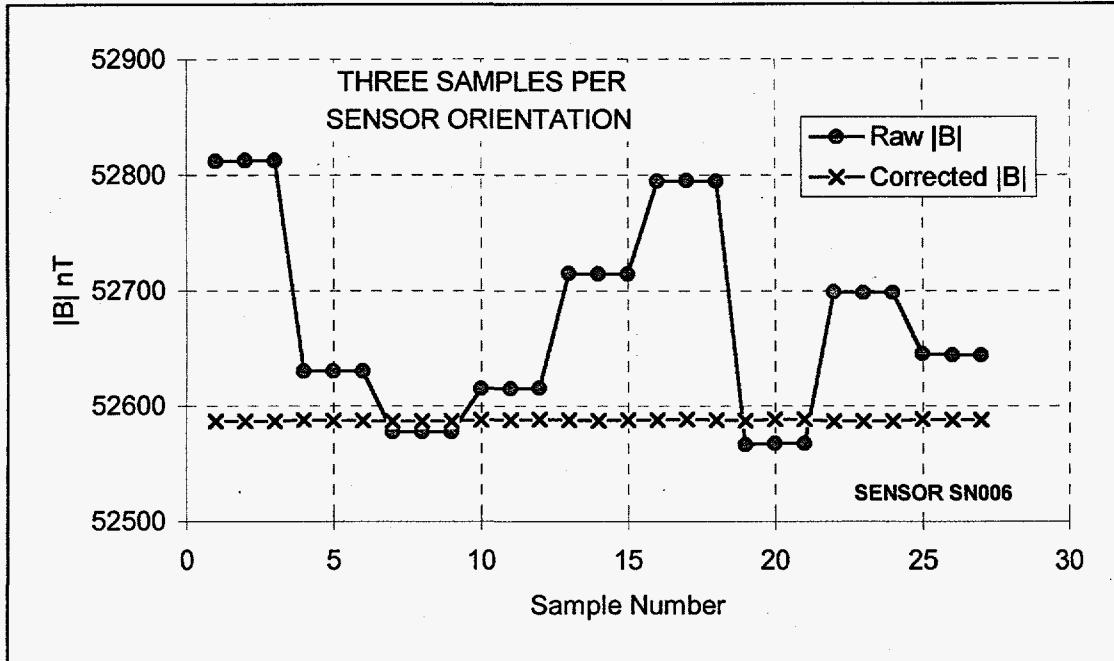


Figure 2-9.  $|B|$  calculated using fluxgate data and using corrected data.

The data transformation can be described in terms of a general vector transformation  $\mathbf{B} = \mathbf{B}_0 + \bar{\mathbf{T}}\mathbf{B}'$ , where:

$$\mathbf{B}' = \begin{bmatrix} B'_x \\ B'_y \\ B'_z \end{bmatrix} = \text{raw fluxgate field vector,} \quad \mathbf{B}_0 = \begin{bmatrix} B_{x0} \\ B_{y0} \\ B_{z0} \end{bmatrix} = \text{field offset vector,}$$

$$\mathbf{B} = \begin{bmatrix} B_x \\ B_y \\ B_z \end{bmatrix} = \text{true field vector, and} \quad \bar{\mathbf{T}} = \begin{bmatrix} t_{11} & t_{12} & t_{13} \\ t_{21} & t_{22} & t_{23} \\ t_{31} & t_{32} & t_{33} \end{bmatrix} = \text{transform tensor.}$$

The absolute value of the true magnetic vector ( $|B|$ ) can be expressed in terms of the measured field ( $B'$ ) and the transformation constants  $\mathbf{B}_0$  and  $\bar{\mathbf{T}}$ , as:

$$|B| = C_0 B_x^2 + C_1 B_y^2 + C_2 B_z^2 + C_3 B_x B_y + C_4 B_y B_z + C_5 B_z B_x + C_6 B_x + C_7 B_y + C_8 B_z + C_9,$$

where the coefficients  $C_k$  are functions of the elements  $B_{i0}$  and  $t_{ij}$ . The coefficients are determined during a magnetometer alignment procedure in which  $B'$  data are recorded for multiple sensor orientations while in a constant magnetic field. The coefficients are then numerically found by a least-squares method. After the polynomial coefficients are determined, they are coded into the BC software. The polynomial transformation substantially reduces heading error as indicated in Figure 2-9.

Advantages of the fluxgate total field magnetometer over conventional total field magnetometers are its light weight and high update rate. The primary disadvantage is that the readings can drift with temperature due to the thermal properties of fluxgate cores. The magnitude of drift that we

experienced, however, has been too small to effect our surveys. Properties of the total field fluxgate magnetometer are listed in Table 2.

**Table 2. Specifications of the GAUSS fluxgate total-field magnetometer.**

|                                     |                                |
|-------------------------------------|--------------------------------|
| Thermal drift                       | < 1.5 nT/°C in 50,000 nT field |
| Weight (all electronics & sensor)   | 9.5 oz                         |
| Update rate (raw vector data)       | 240 sec <sup>-1</sup> max.     |
| Update rate (corrected total field) | 4 sec <sup>-1</sup> max.       |
| Resolution                          | < 1 nT                         |
| Heading error (worst case)          | < 20 nT                        |

### 2.2.2 Electromagnetic Induction Instrument

Geophex has been involved with EM instrument research for more than 10 years. During this research project, we enhanced our state-of-the-art EM instrument electronic systems for use with the GAUSS. The areas that we addressed to create a GAUSS-compatible instrument were:

1. Replace discrete logic with programmable logic array devices, when possible,
2. Reduce circuit complexity by performing more functions with CPU,
3. Replace hand-wired protoboards with printed circuit boards (PCB) to improve reliability,
4. Modify system to operate from a unipolar voltage supply,
5. Reduce system baseline drift,
6. Allow software selectable waveform generation (resulting in a broadband instrument), and
7. Modify software and hardware for real-time transmission of data.

Brief descriptions of the electronic components and physical characteristics of our EM instrument are presented in Sections 2.2.2.1 and 2.2.2.2, respectively. Additional details of the EM instrument and methodology is presented in Appendix F.

#### 2.2.2.1 Electronic Assembly

The goals listed above were successfully completed, resulting in an EM electronics assembly that uses a single 9 cm by 21 cm PCB, weighs less than 0.4 kg, and is powered by a single battery pack. By comparison, the previous design required three circuit boards, heavy, unreliable interboard connections, and three separate battery stacks.

A basic block diagram of the GAUSS EM induction sensor system is shown in Figure 2-10. The system is comprised of an electronics console and a coil assembly. Electronic systems are controlled by a proprietary high performance computer based on the Motorola 56001 digital signal processing (DSP) chip. During operation, a synthesized voltage waveform is applied to the transmit (Tx) coil. The Tx-coil current produces a strong primary electromagnetic field. If a conductive object is in the vicinity, this primary field will induce electric current in that object. The induced current gives rise to secondary electromagnetic fields which, in turn, generates

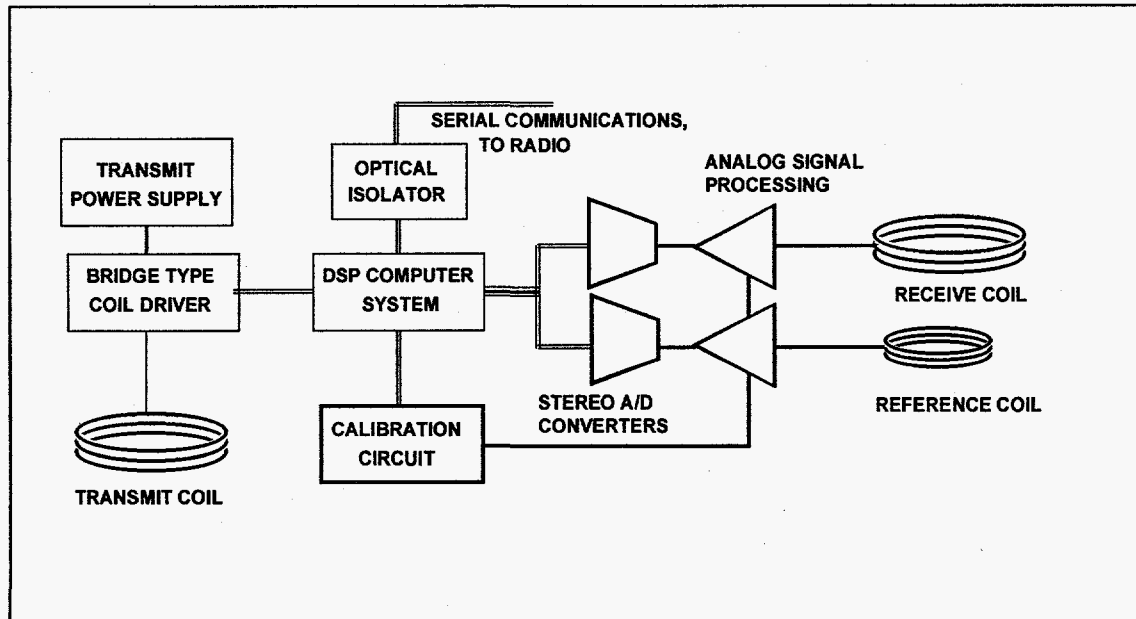


Figure 2-10. A simplified block diagram of the GAUSS electromagnetic sensor system.

potential across the receiver (Rx) coil. Changes in Rx coil voltage are detected and indicate changes in conductivity of the surroundings. The Rx coil signal is of small magnitude and is processed by precision, low-noise analog circuitry which supplies appropriate filtering and amplification. The receiver is broad-band, allowing multifrequency operation.

Because the instrument is battery powered, the transmit field strength decreases during use due to battery voltage decay. A reference coil (Bx) is located to monitor the Tx coil field strength. We use this ratio for target detection because the Rx/Bx signal ratio is not effected by Tx signal strength.

The Tx voltage waveform is synthesized using a pulse width modulation (PWM) scheme. The computer produces a bitstream which controls a tri-state bridge circuit. The bridge modulates the transmit supply voltage and produces a PWM voltage waveform. The advantage of this transmitter is that the computer bitstream is easily modified to produce any desired waveform, resulting in multifrequency operation. Lower frequencies are able to penetrate deeper into the Earth while higher frequencies are useful in detecting shallower objects.

After analog processing, the Rx and Bx signals are digitized by a Crystal CS5336 stereo A/D converter at 36.45 kilosamples per second per channel. The DSP computer then cross correlates each recorded, digitized waveform with the sine and cosine components of the transmitted waveform for each selected frequency. This process provides both amplitude and phase information for target anomalies. Software for the DSP computer is written primarily in assembly language because very tight timing requirements are required. The computer must maintain synchronization while simultaneously transmitting a control sequence to the Tx coil driver, controlling and reading the A/D converter, and performing signal processing on the Rx and Bx

channel data. Additionally, the EM system sensing circuits must be inactive during radio transmission of the telemetry system to avoid interference.

#### 2.2.2.2 Physical Description of the EM Instrument

The EM instrument consists of two parts: the electronics console and the coil housing. The electronic components, including the battery pack, circuit board, and computer, are housed in an aluminum console. The total weight of the console is 5.4 pounds. The console is electrically grounded and shielded to minimize environmental noise.

The transmit, receive, and bucking coils are housed in a ski that is made of balsa wood with Kevlar skin. The Kevlar housing is constructed out of a single piece of material to minimize differential, thermal-induced expansion and contraction. The total weight of the housing and coils is 4.5 pounds.

The primary limitation to using our EM instrumentation is system weight. The model helicopter platform does not have enough payload capacity to carry our EM instruments. Because GAUSS is not limited to model helicopters, however, we pursued alternative platforms that can carry the required payload. These alternative platforms are described in Section 2.1.5.2.

#### 2.2.3 Altimeter

The GAUSS uses a commercial ultrasonic sensor, manufactured by Polaroid, to measure altimetry data. The altimeter sensor, which consists of an acoustical transducer and ranging circuit electronics, weighs only a few ounces.

The ultrasonic ranging unit consists of two components; an acoustical transducer (Environmental Grade, model 6500) and ranging circuit board (Figure 2-11). These components can detect the presence and distances of objects within a range of 0.5 to 35 feet. The typical absolute accuracy is  $\pm 1$  percent of the reading. The transducer is powered by a single battery with a supply voltage of between 4.5 and 6.8 v and designed for operation in temperatures that range from 0 to 40°C. In operation, a pulse is transmitted toward a target and the resulting echo is detected by the transducer. The timing of the signal is performed by the 5F-LCD onboard computer. The elapsed time between initial transmission and echo detection is then converted to distance by the BC.

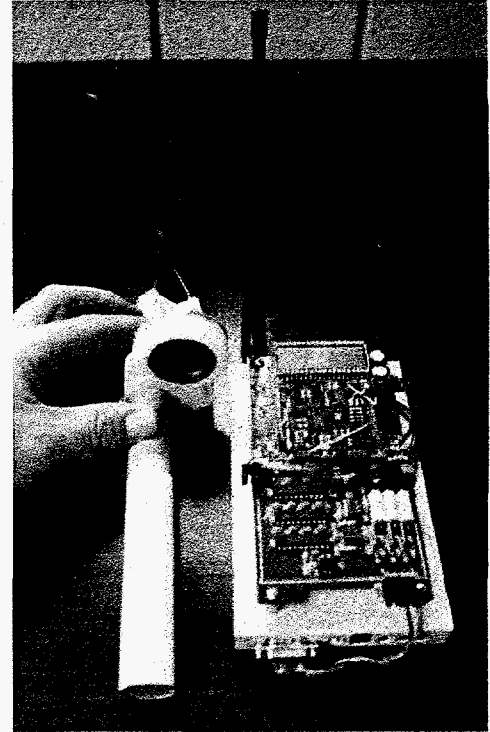
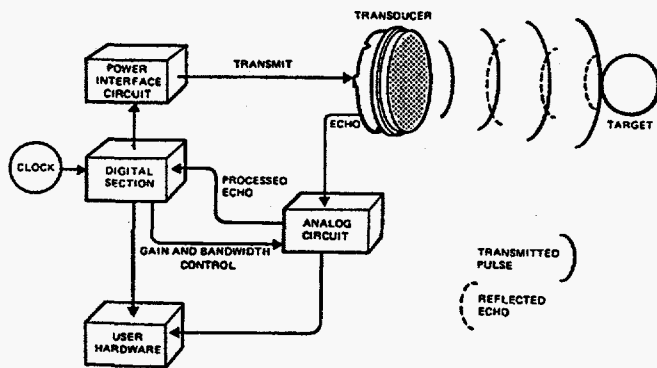


Figure 2-11. Block schematic of the Polaroid altimeter sensor (left). Photograph on the right shows the altimeter fastened to the Fluxgate magnetic sensor, processing circuitry, and RF modem that is used in the GAUSS.

### 3.0 Test and Evaluation

This section describes a typical sequence of events for a geophysical survey using the GAUSS and presents the acquired data.

#### 3.1 Logistics

Figure 3-1 shows the GAUSS hardware components. The laptop computer and RF modem are located on the temporary table. The ROH and its magnetometer payload is observed in the foreground. The Geodimeter is positioned on the left side of the photo.

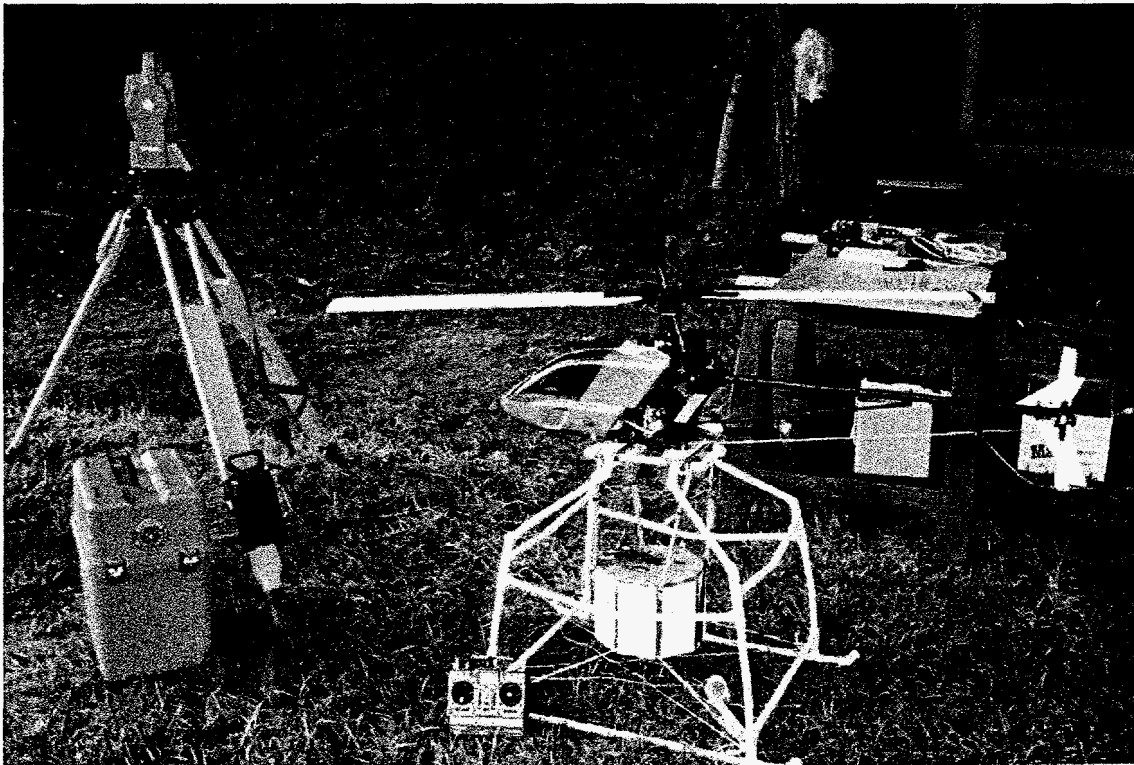


Figure 3-1. Photograph of the GAUSS hardware prior to a test survey.

After the UAV platform is ready for flight and the geophysical sensors are turned on, the SCS is started by typing the executable filename, "GAUSS". Figure 3-2 shows the screen of the BC prior to setting the limits of the survey area during a magnetic survey.

Setup procedures include verifying that the sensor and position data are being properly received and defining the limits of the survey area. To define the limits of the site, the users must position the UAV at three locations along the site perimeter as shown in Figure 3-3.

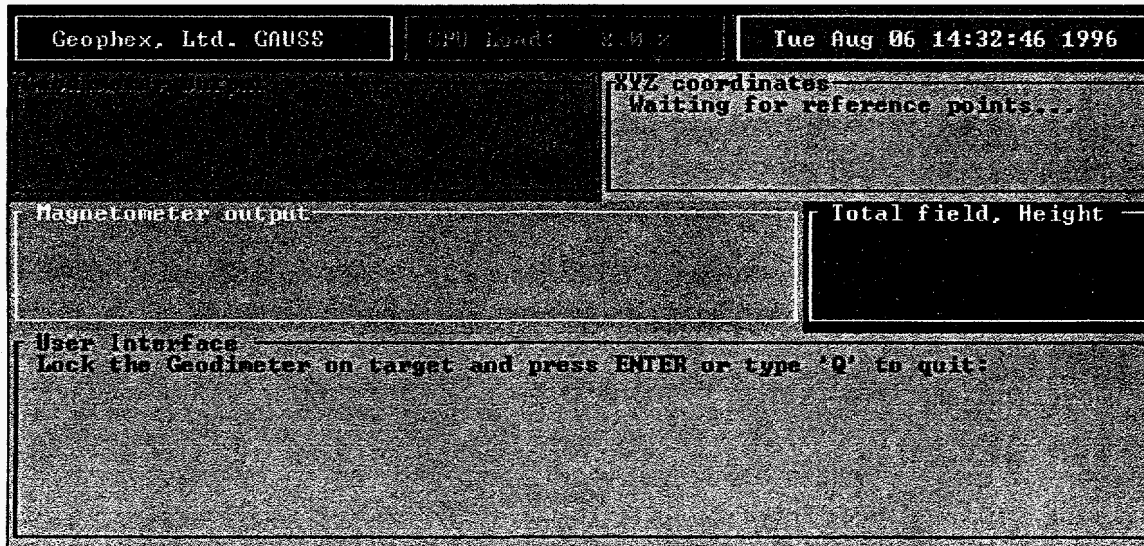


Figure 3-2. Image of the base station screen prior starting the instruments.

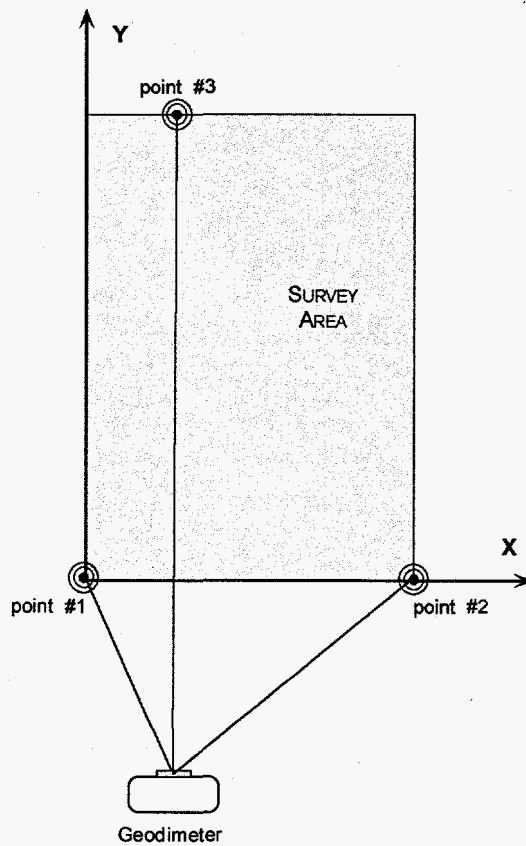


Figure 3-3. Three reference points are necessary for establishing the transformation from the spherical coordinate system used by the Geodimeter to the rectangular system.



Upon successful completion of this phase, the SCS displays the information shown in Figure 3-4. As seen in Figure 3-4, the surveyors can verify the status of the positioning system (upper left), coordinates of the UAV (upper right), FC output (middle left), and sensor measurements (middle right) prior to starting the survey.

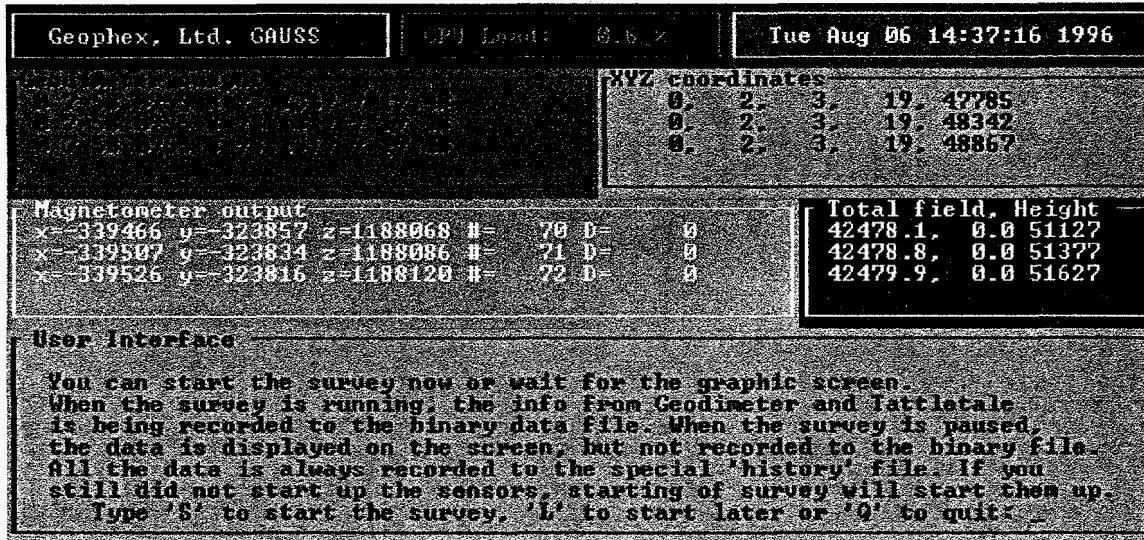


Figure 3-4. Image of the base station screen after the data links are established and the limits of the site are defined.

After the data integrity is verified, the user enters the graphics mode to initiate the survey (Figure 3-5). Although the example screen shown in Figure 3-5 is for a magnetic survey, the “windows” for the electromagnetic sensor serve similar functions. The purpose of each window shown in Figure 3-5 is:

| <u>Window</u> | <u>Function</u>                                                                                                                                                                                                          |
|---------------|--------------------------------------------------------------------------------------------------------------------------------------------------------------------------------------------------------------------------|
| 1             | Geophex title,                                                                                                                                                                                                           |
| 2             | Dynamic load of the central processor,                                                                                                                                                                                   |
| 3             | Survey date and time,                                                                                                                                                                                                    |
| 4             | Displays the data link between the BC and the peripheral devices. The yellow lines indicate receipt of data and scroll upward as time progresses - a qualitative analysis of the data update rate,                       |
| 5             | Battery voltage on the remote UAV-towed sensor package,                                                                                                                                                                  |
| 6             | Number of data points acquired,                                                                                                                                                                                          |
| 7             | Number of computer-screen snapshots recorded to disk,                                                                                                                                                                    |
| 8             | Value of the most recent geophysical data,                                                                                                                                                                               |
| 9             | Altimeter height (in feet),                                                                                                                                                                                              |
| 10            | Display of the current color scale and dynamic display capabilities: including, the area shown on the screen (below color scale), number of pixels used to represent data point, redraw option, and interpolate command, |
| 11            | General command listing and hot-key information, and                                                                                                                                                                     |
| 12            | Screen map of the survey area.                                                                                                                                                                                           |

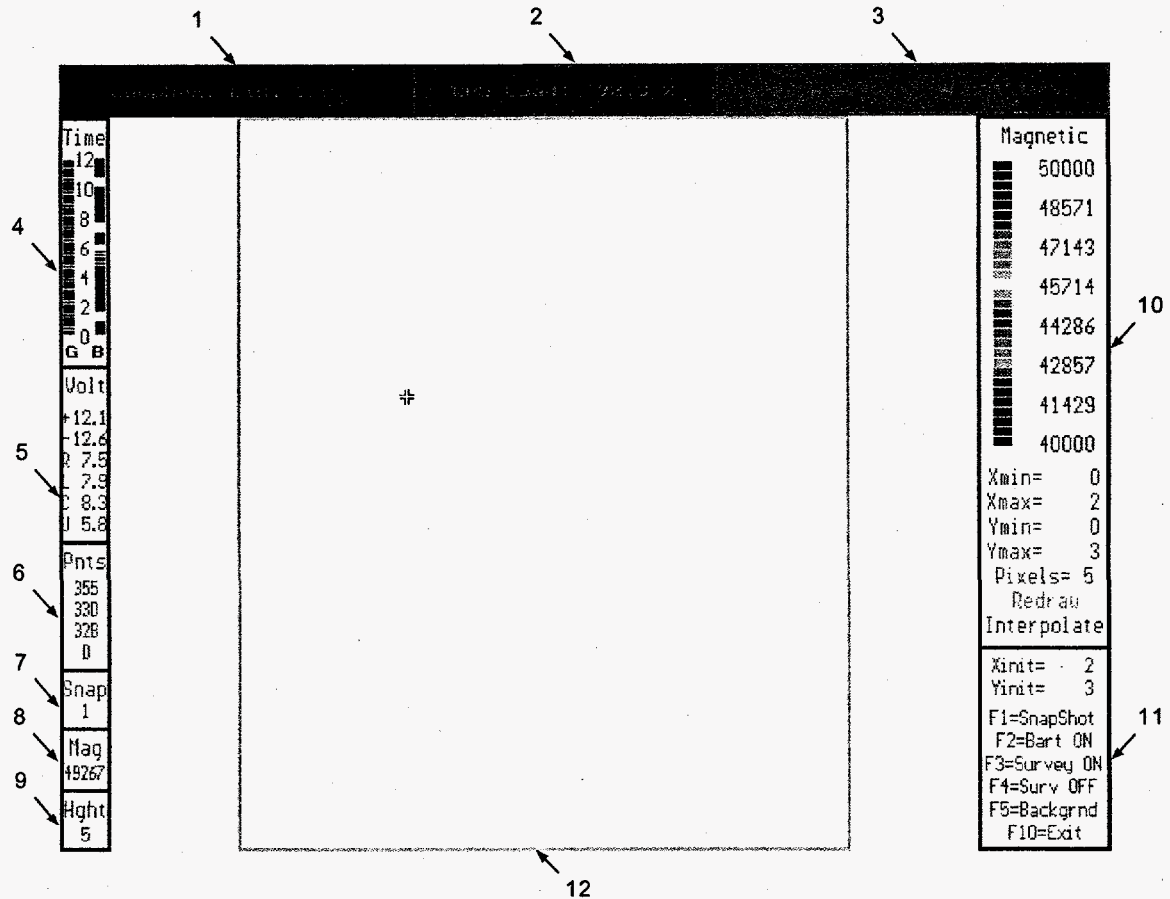


Figure 3-5. Typical appearance of the graphics screen immediately after entering the graphics mode (just prior to surveying). The purpose of each window is explained in the text.

### 3.2 Geophex Geophysical Test Site

In November 1994, Geophex constructed a 1/4 acre geophysical test site (Figure 3-6). The site features targets buried at known depths and orientations. The site presents a challenging, realistic location for geophysical sensing. A chain-link fences borders the west side, vegetation borders the north, and a metal building is located near the southern site border.

Details of the subsurface targets are provided in Figure 3-7. The storm drain system uses 2-ft diameter reinforced concrete pipe for the north-south leg. The center of the pipe is approximately 4.5 ft deep. The east-west leg of the storm drain uses two types of pipe; a one-ft diameter ceramic pipe is buried at a depth of 3.5 ft west of the vault and a one-ft-diameter reinforced concrete pipe is buried at a depth of 4 ft east of the vault.

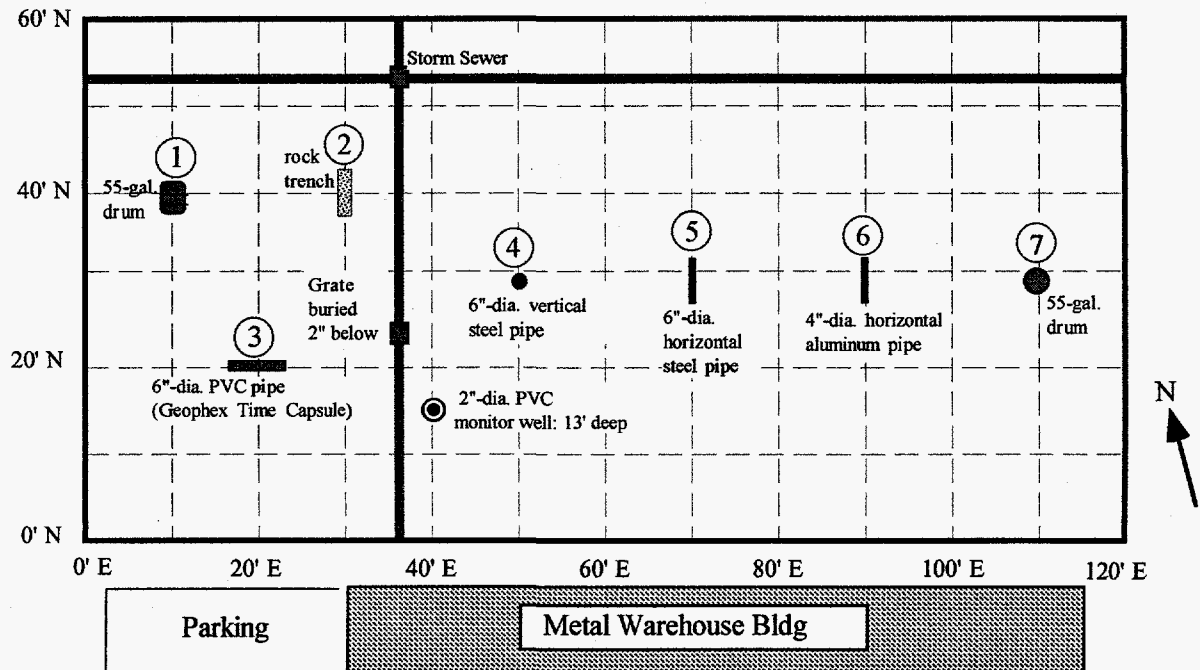


Figure 3-6. Location of buried targets within the Geopex geophysical test facility. Descriptions of the targets are provided in Figure 3-7.

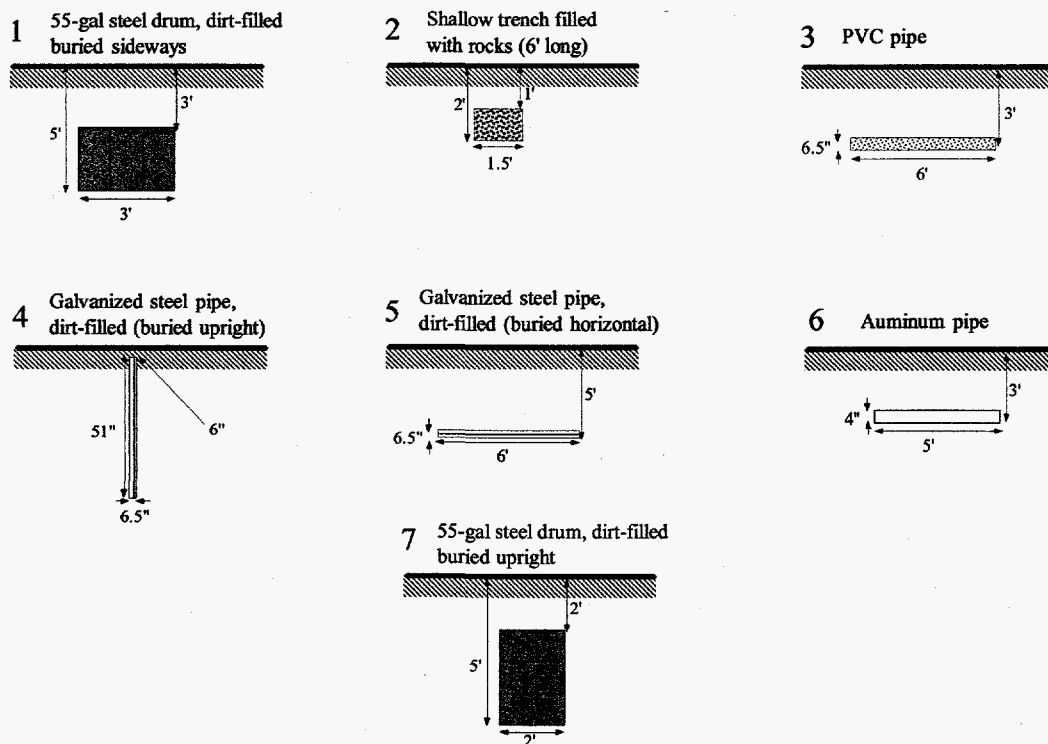


Figure 3-7. Description of buried targets within the Geopex geophysical test facility. See Figure 3-6 for target location.

### 3.3 Demonstration Data

The data presented in this section were acquired at the Geophex Geophysical Test Facility to compare the data quality, quantity, and speed of acquisition between the GAUSS versus man-portable methods. All presented data were acquired within a 24-hour time window to minimize variations in the environmental conditions (viz., rain).

#### 3.3.1 Magnetic Sensor

Section 3.3.1.1 presents data acquired using the prototype fluxgate-magnetometer sensor (i.e., man-portable). Data shown in Section 3.3.1.2 were acquired using the GAUSS and its associated fluxgate-magnetometer sensor package.

##### 3.3.1.1 Fluxgate Magnetometer Data acquired using a Hand-held Sensor

Magnetic data were acquired on a 2.5-ft grid using a hand-held fluxgate magnetometer (Figure 3-8). Two field personnel acquired 1,225 data points in 65 minutes.

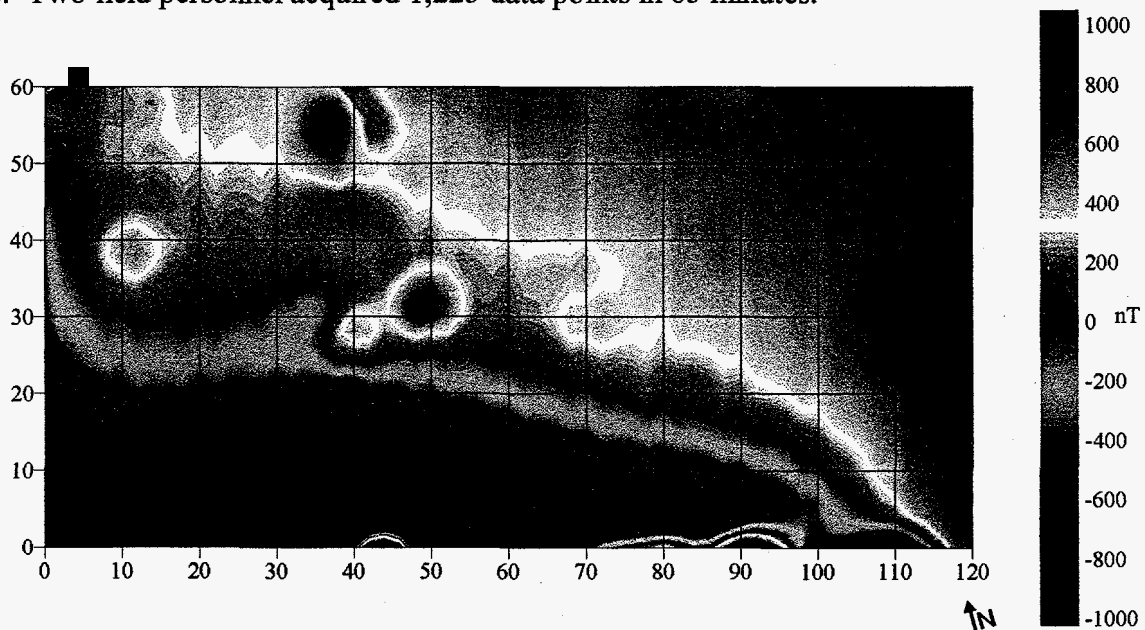


Figure 3-8. Magnetic data acquired using the hand-held fluxgate magnetometer.

### 3.3.1.2. GAUSS Magnetometer Data

Magnetic data were acquired using the GAUSS and the ROH (Figure 3-9). Snapshots of the BC computer screen (Figure 3-10 to 3-14) demonstrate the flexibility and value of the real-time survey-control software. During the survey, the BC operator instructed the ROH pilot where to acquire additional data. We acquired over 4,500 data points in less than 60 minutes. Data from three sorties, required to adequately cover the entire test area due to a limited amount of fuel, were automatically combined by the SCS.

To properly compare the GAUSS-acquired magnetic data with data acquired using hand-held instruments, we post-processed the two data sets using identical procedures. Figure 3-14 shows the resulting magnetic data that was acquired using the GAUSS and the ROH. Comparisons of Figure 3-14 and Figure 3-8 are remarkably similar.

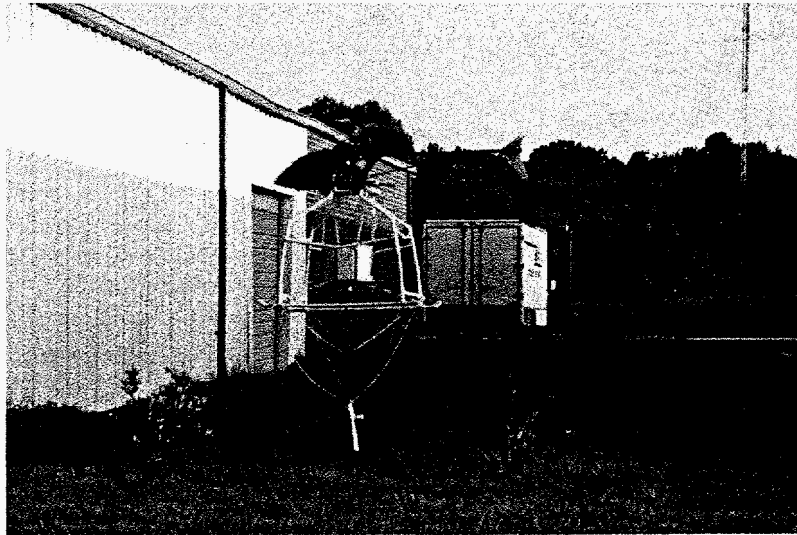


Figure 3-9. Photograph of the ROH and magnetic sensor package during data acquisition.

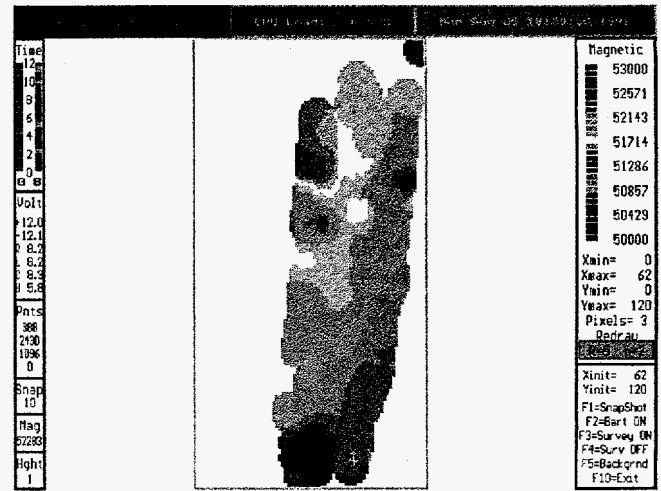
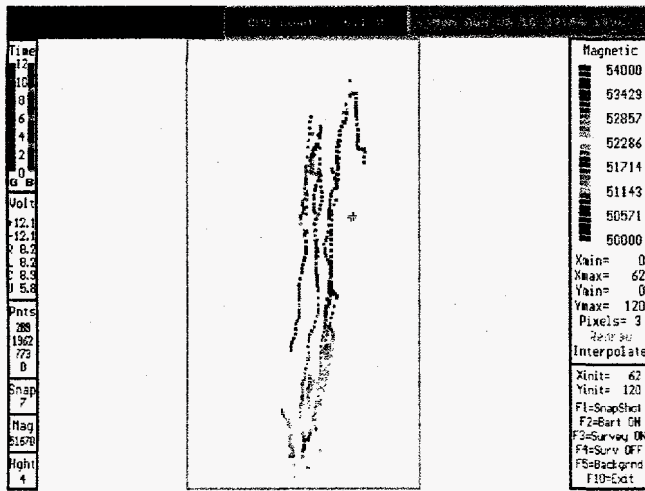


Figure 3-10. Snapshot of the BC screen near the beginning of the magnetic survey using the GAUSS: left side -magnitude and location of individual data points; right side - interpolated map.

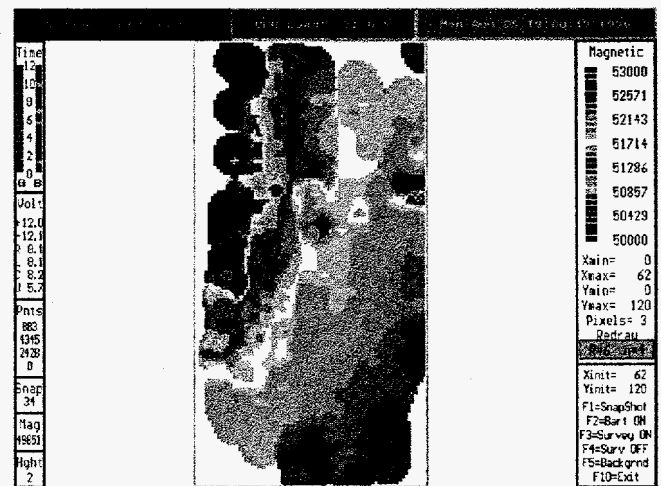
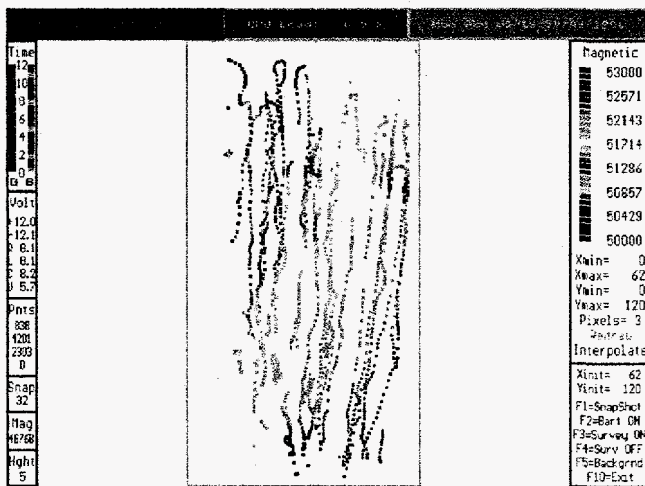


Figure 3-11. Snapshot of the BC screen near the middle of the magnetic survey using the GAUSS: left side - magnitude and location of individual data points; right side - interpolated map.

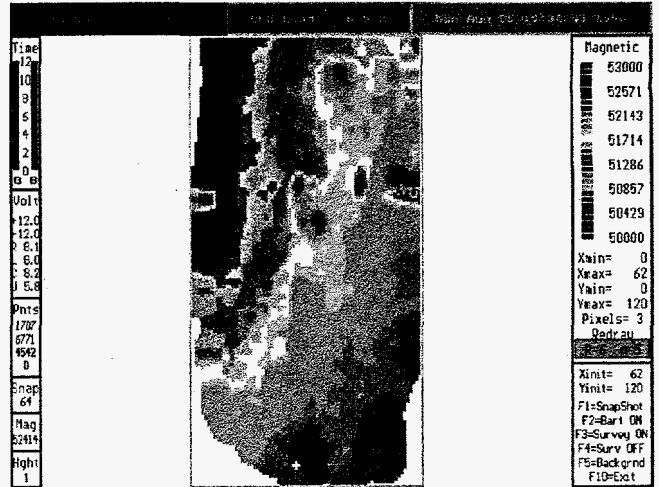
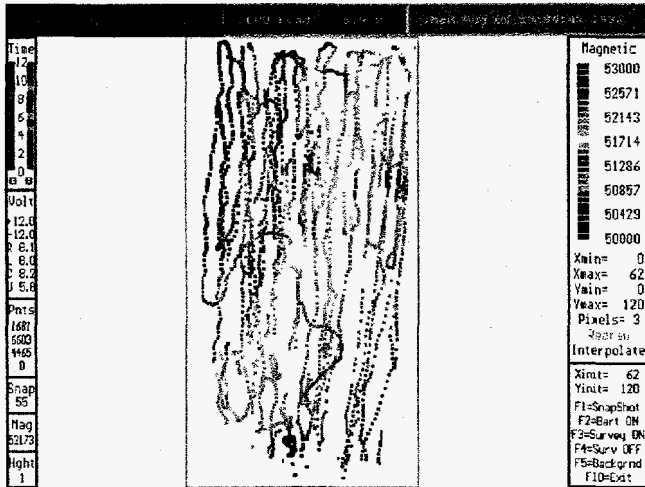


Figure 3-12. Snapshot of the BC screen near the end of the magnetic survey using the GAUSS: left side - magnitude and location of individual data points; right side - interpolated map.

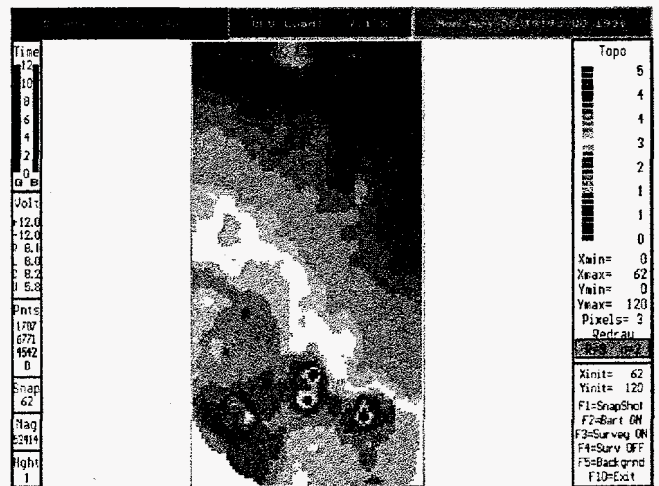


Figure 3-13. Topographic map produced during the magnetic survey: left side - magnitude and location of individual data points; right side - interpolated map.

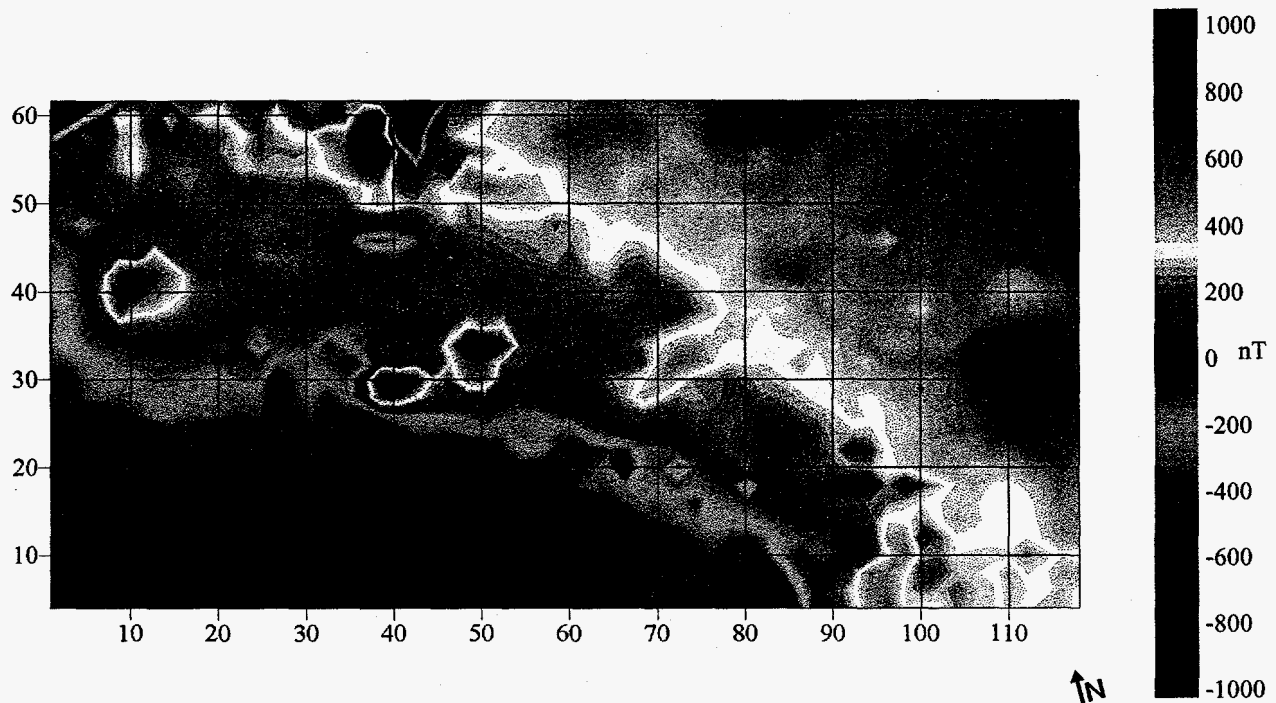


Figure 3-14. Magnetic data acquired using the GAUSS. The data were post processed and contoured for direct comparison to Figure 3-8.

### 3.3.2 Electromagnetic Sensor

Section 3.3.2.1 presents data acquired using man-portable EM instrument (survey positions are recorded using the “dead reckoning” method). Data shown in Section 3.3.2.2 were acquired using the GAUSS. Because the ROH cannot carry the EM sensor (due only to payload limitations), we manually carried the instrument, but used the GAUSS acquisition hardware and software to record spatial registry and geophysical data. The multifrequency EM sensor was configured to acquire data using two transmitter frequencies (2,430 and 7,290 Hz). Each transmitter frequency produces two maps (viz., in-phase and quadrature components).

#### 3.3.2.2 Man-portable EM Data

Data from a hand-held EM survey are shown in Figures 3-15 to 3-18. Two field personnel acquired 6,800 data points in 60 minutes. The survey lines were spaced 2.5 ft apart. The in-line data spacing is 2 feet. Data processing included assigning spatial registry coordinates, krigging, and contouring.



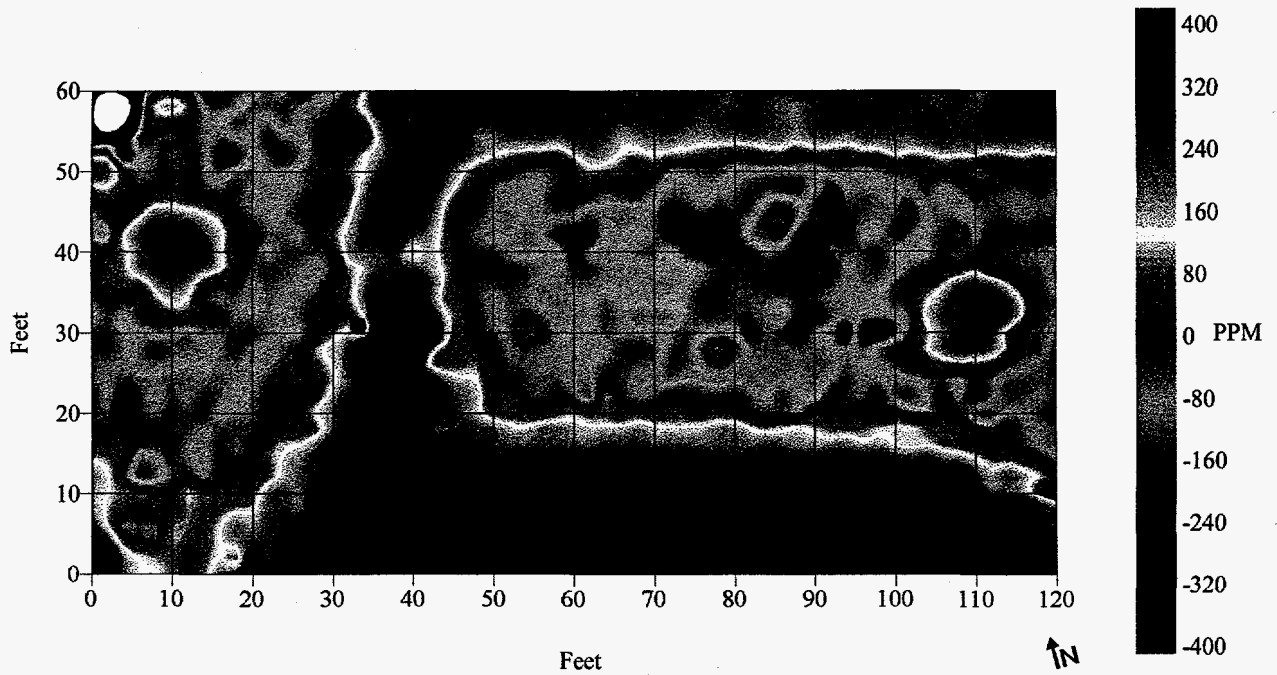


Figure 3-15. Electromagnetic data, 2,430 Hz in-phase component, acquired using a hand-held EM instrument with an internal data logger.

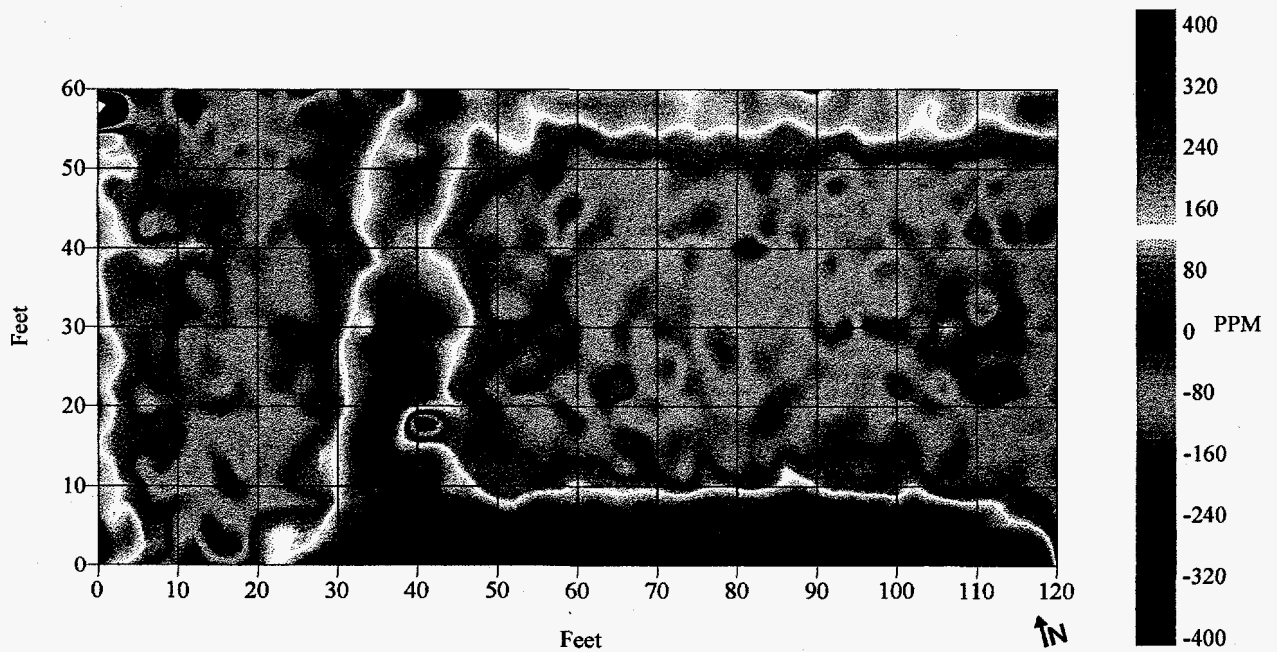


Figure 3-16. Electromagnetic data, 2,430 Hz quadrature component, acquired using a hand-held EM instrument with an internal data logger.

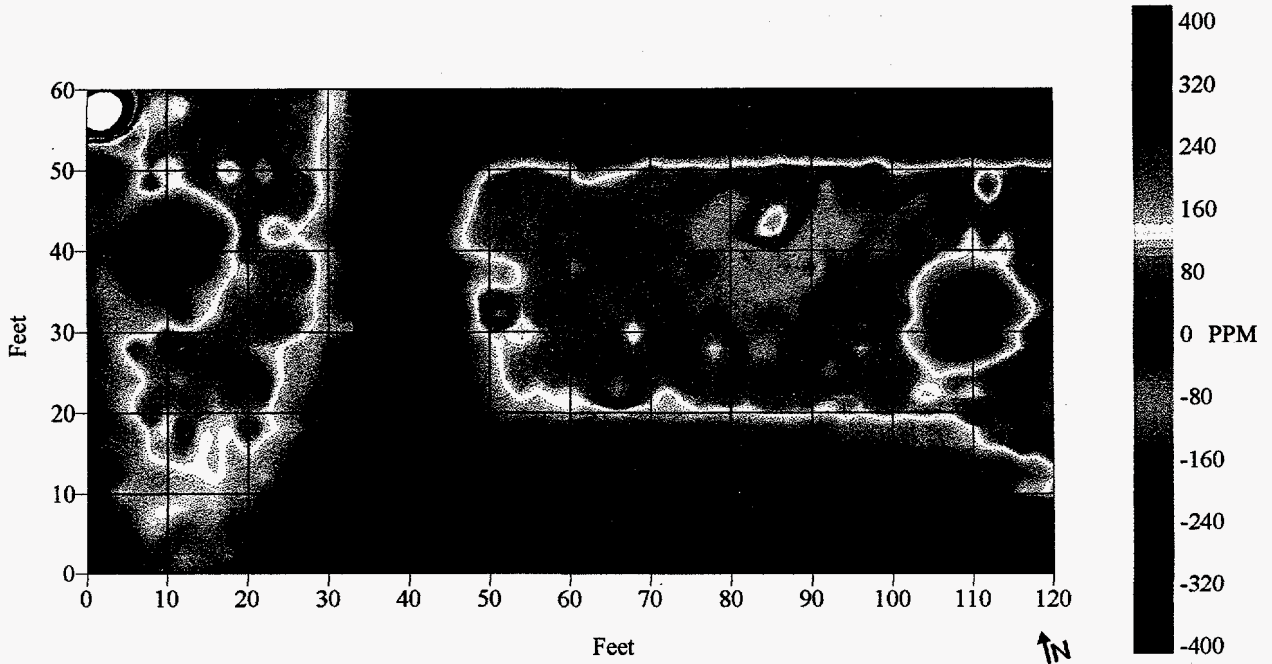


Figure 3-17. Electromagnetic data, 7,290 Hz in-phase component, acquired using a hand-held EM instrument with an internal data logger.

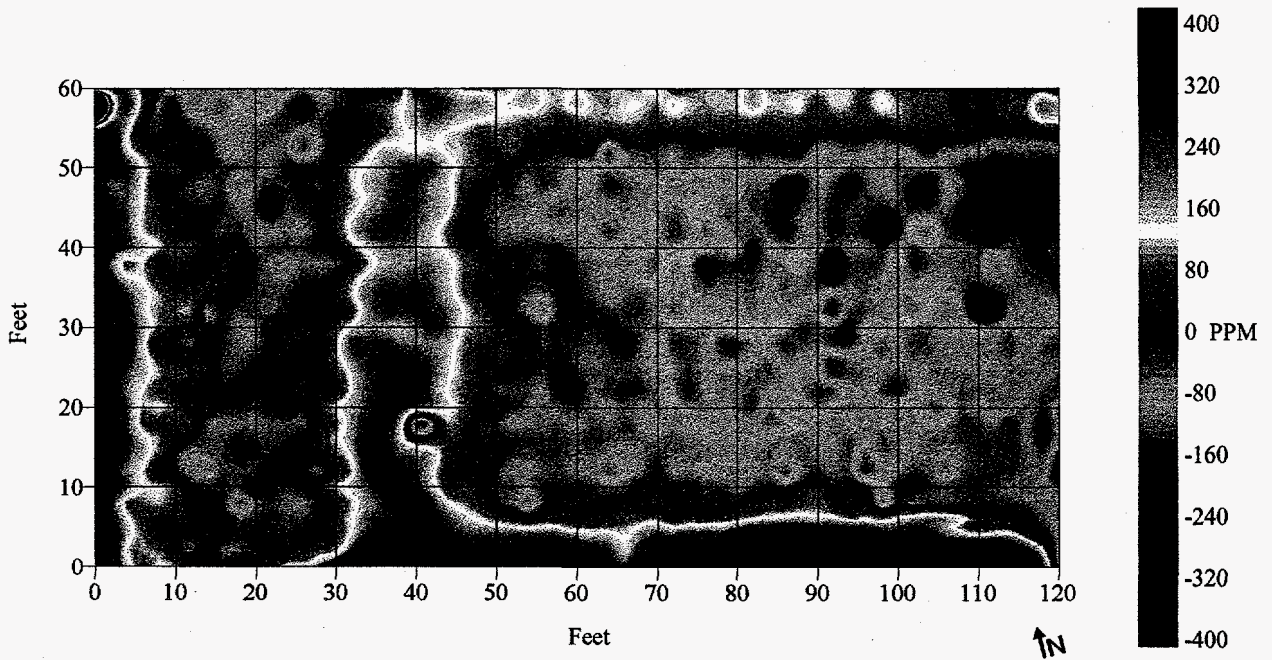


Figure 3-18. Electromagnetic data, 7,290 Hz quadrature component, acquired using a hand-held EM instrument with an internal data logger.

### 3.3.2.2 EM Data acquired using the GAUSS Acquisition Hardware and Software

We acquired EM data using a pseudo-GAUSS configuration. Although the EM instrument was hand-carried because the ROH cannot carry the payload, the GAUSS data-acquisition system was employed to record, process, and display the data. Three field personnel acquired over 10,500 data points in less than 60 minutes.

Figures 3-19 through 3-22 show the progress of the survey as recorded and displayed at the BC. Data shown in Figures 3-23 through 3-26 were post-processed, kriged, and contoured to facilitate data comparisons.

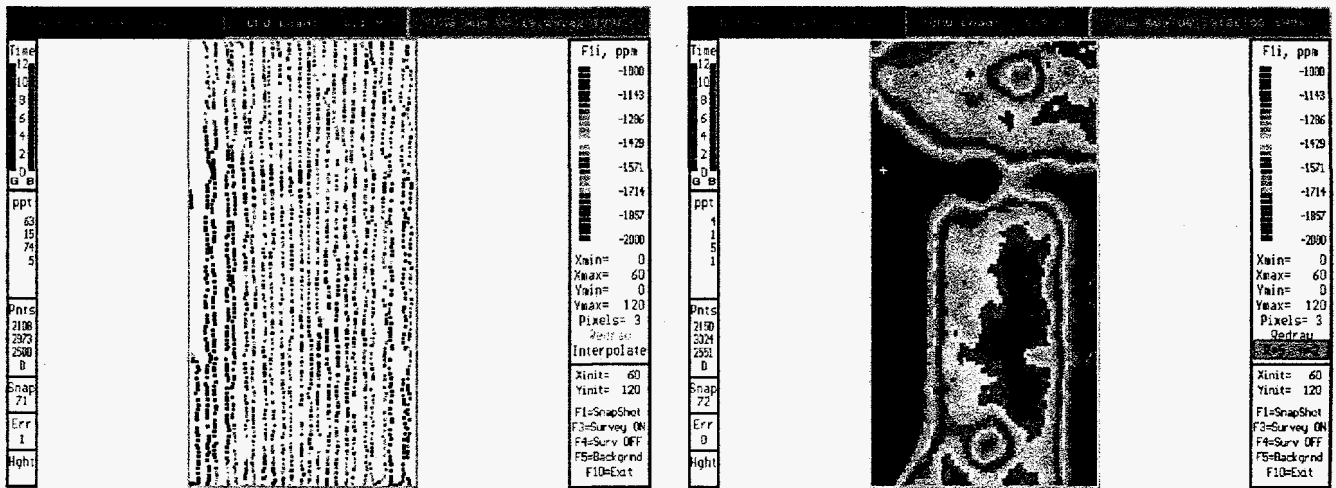


Figure 3-19. Real-time display of the EM data, 2,430 Hz in-phase component, acquired using a hand-held EM instrument and the GAUSS acquisition hardware and software.

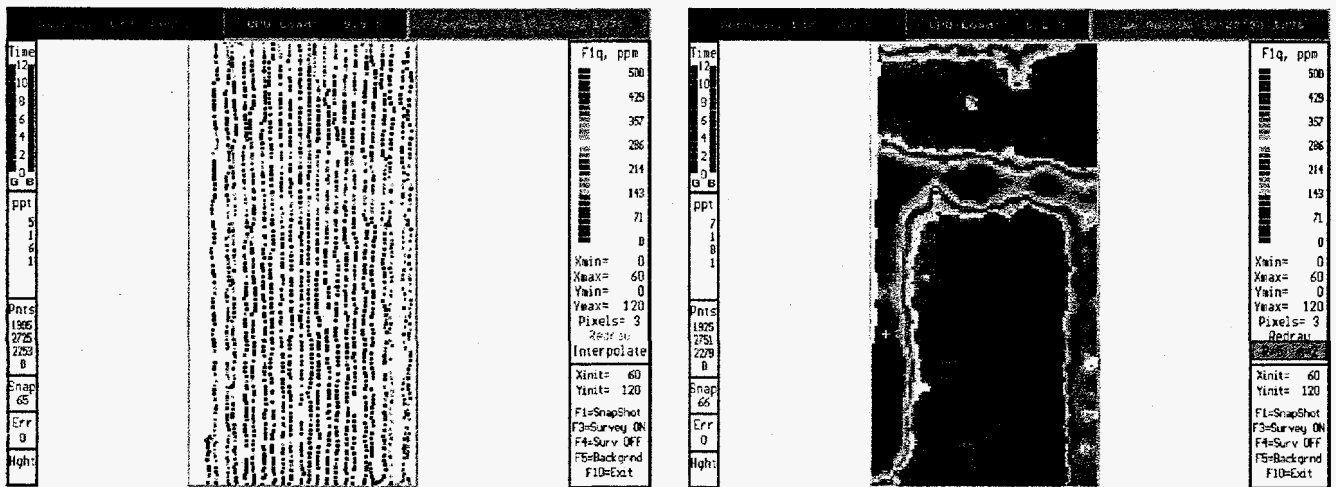


Figure 3-20. Real-time display of the EM data, 2,430 Hz quadrature component, acquired using a hand-held EM instrument and the GAUSS acquisition hardware and software.

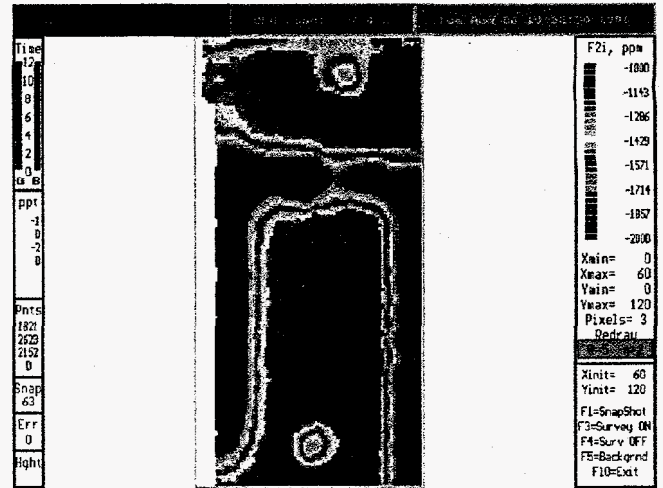
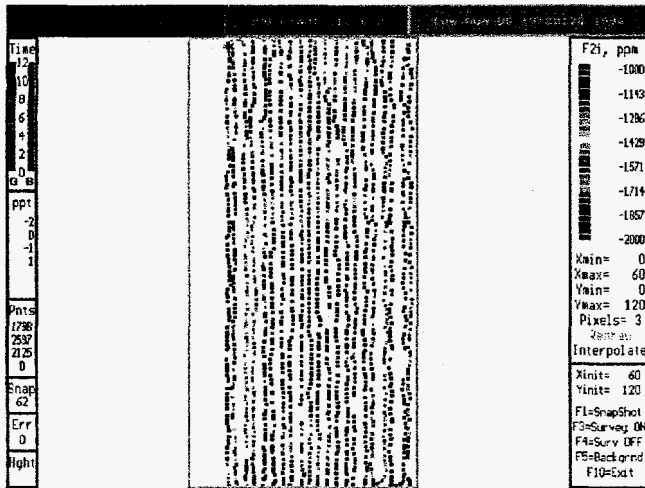


Figure 3-21. Real-time display of the EM data, 7,290 Hz in-phase component, acquired using a hand-held EM instrument and the GAUSS acquisition hardware and software.

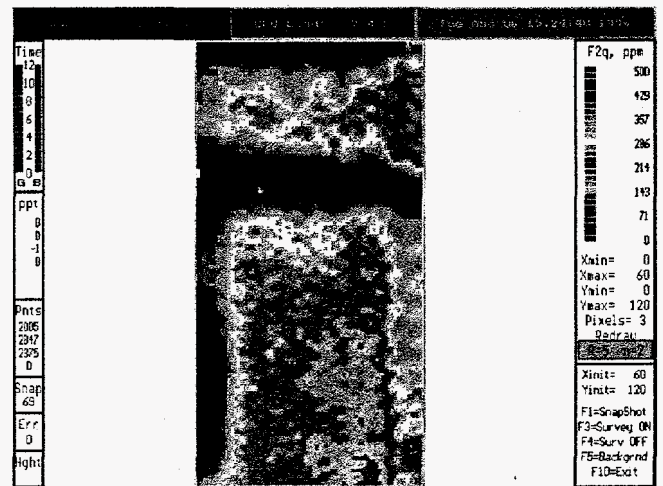
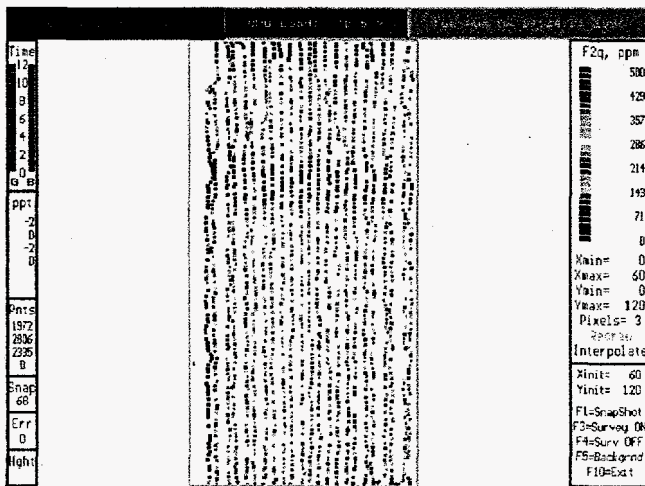


Figure 3-22. Real-time display of the EM data, 7,290 Hz quadrature component, acquired using a hand-held EM instrument and the GAUSS acquisition hardware and software.

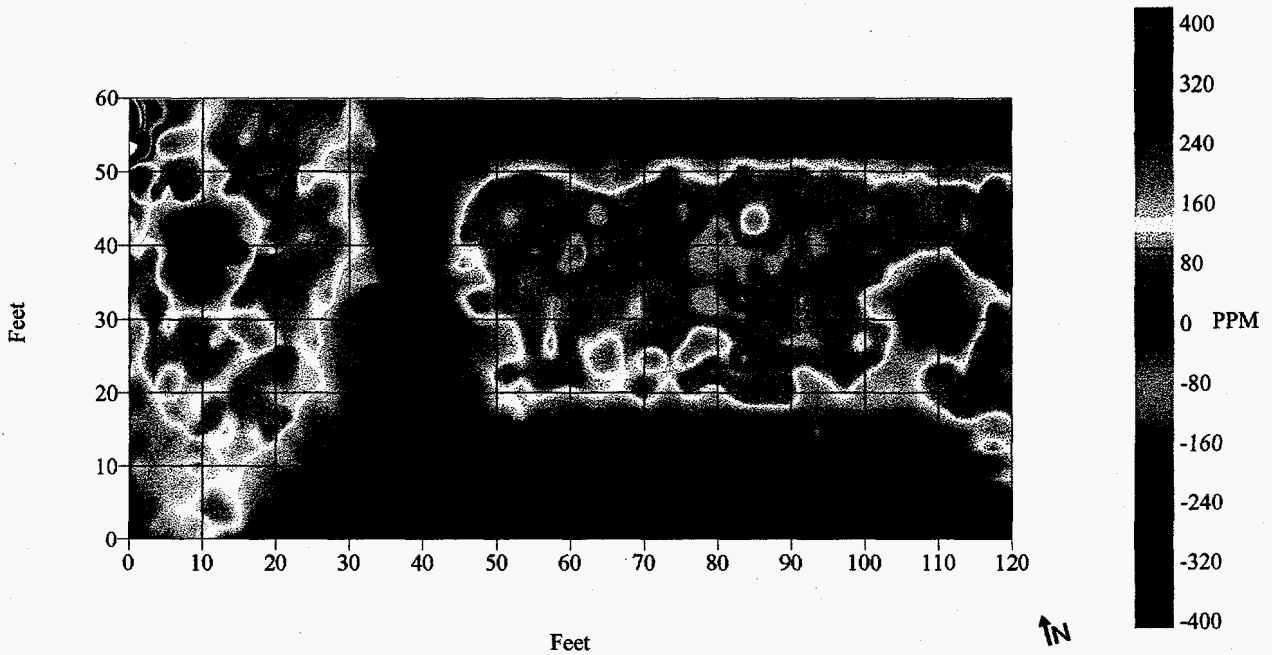


Figure 3-23. Post-processed EM data, 2,430 Hz in-phase component, acquired using a hand-held EM instrument and the GAUSS acquisition hardware and software.

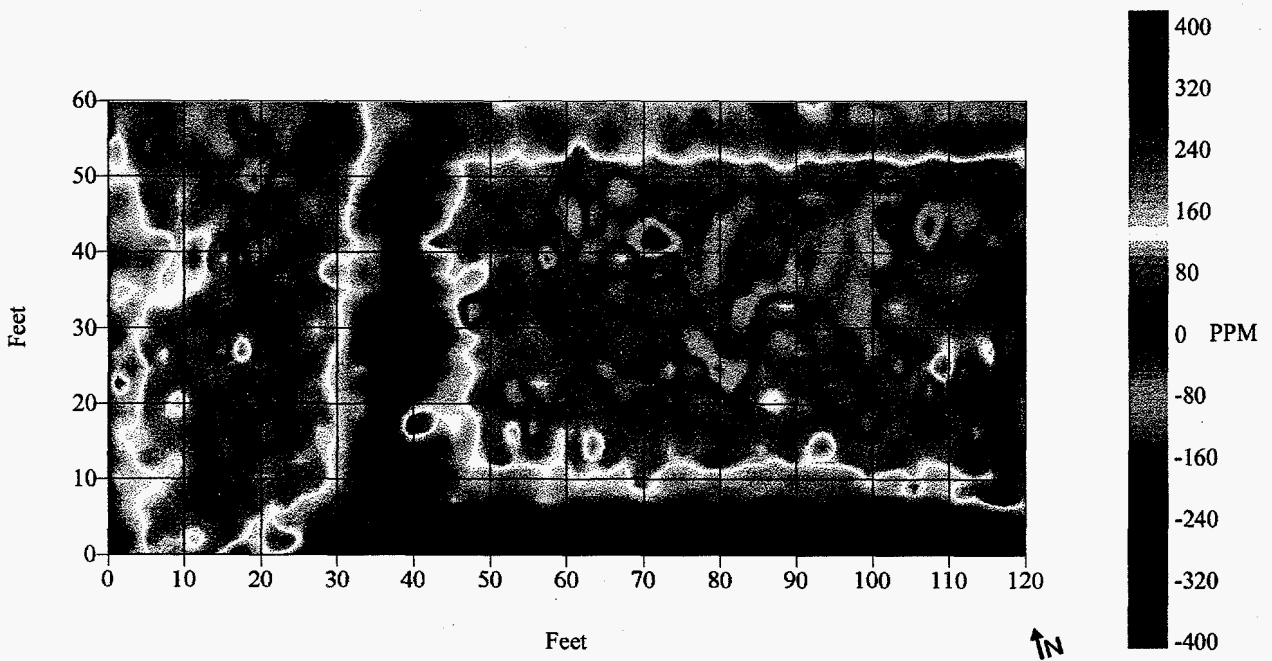


Figure 3-24. Post-processed EM data, 2,430 Hz quadrature component, acquired using a hand-held EM instrument and the GAUSS acquisition hardware and software.

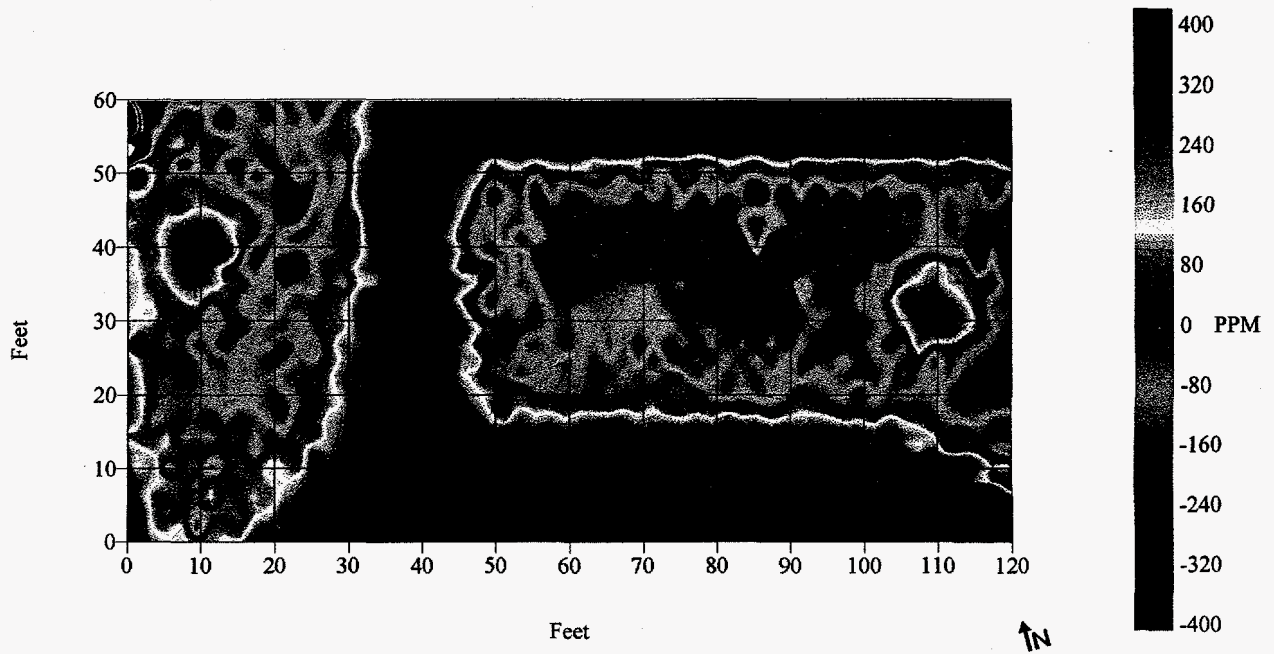


Figure 3-25. Post-processed EM data, 7,290 Hz in-phase component, acquired using a hand-held EM instrument and the GAUSS acquisition hardware and software.

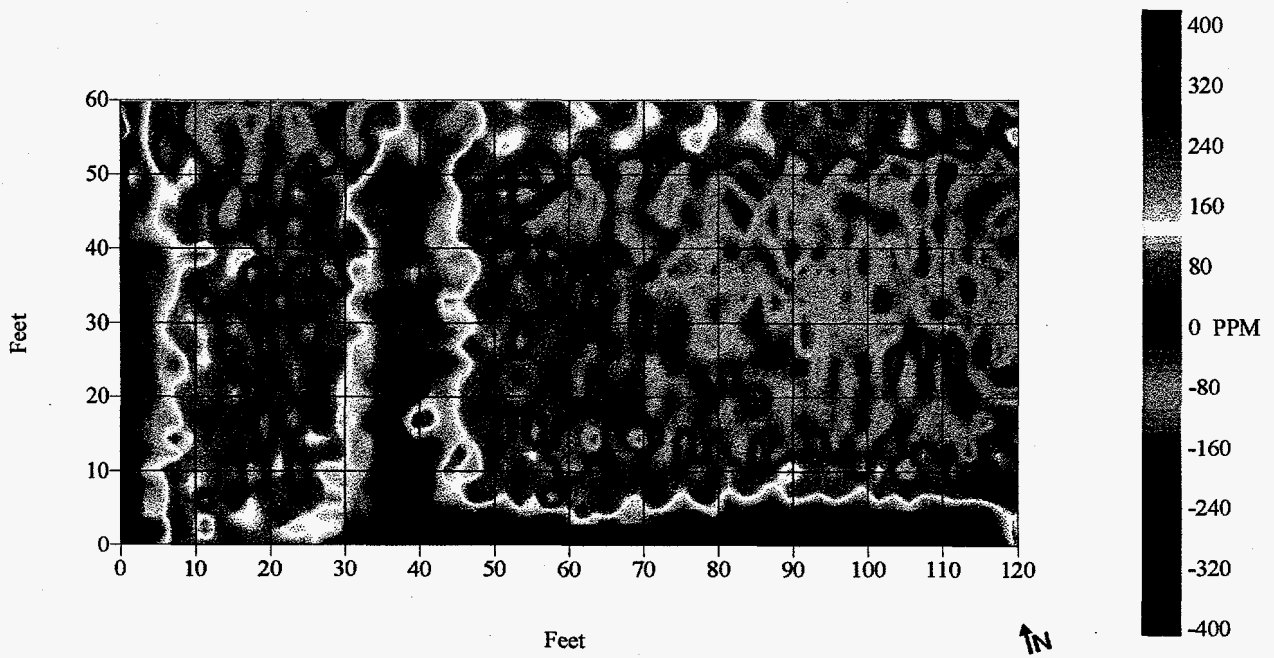


Figure 3-26. Post-processed EM data, 7,290 Hz quadrature component, acquired using a hand-held EM instrument and the GAUSS acquisition hardware and software.

## 4.0 Discussion

Assessing subsurface conditions is an important component of geophysical site assessment and remediation programs. The GAUSS provides a data-acquisition method that is faster, better, cheaper, and safer than is possible using man-portable equipment at sites containing hazardous or radioactive waste materials. The key environmental objectives this program addressed involve reducing data-acquisition costs and survey time, increasing personnel safety, and enhancing the speed and quality of the interpretations.

The ability of UAVs to operate over difficult terrain or dangerous conditions provides many potential applications for the system. The GAUSS has a variety of environmental applications at DOE's nuclear, biological, and chemical waste sites as well as ordnance and explosive waste (OEW) sites. The GAUSS could be tailored for applications in battlefields for locating and neutralizing buried mines on land, beach, and surf zone. The low cost of this system, high data-acquisition rate, and real-time display make it a viable alternative to present technologies.

The GAUSS is comprised of subsystems that can operate either independently or collectively using error-checking protocols. This modularity allows the GAUSS to be changed by modifying or replacing any subsystem if new technology or subsystems become available. The fundamental subsystems include the:

- survey platform (UAV),
- geophysical sensors,
- position measurement subsystem,
- telemetry subsystem,
- base station computer (BC), and
- survey control software (SCS).

Numerous field tests, flight tests, and system tests were conducted to determine the efficiency, reliability, and accuracy of the GAUSS. Based on these tests, we believe the strengths of the GAUSS include the:

- modularity of the hardware systems and software algorithms,
- robust survey-control software,
- real-time display and interpretational features, and
- field-efficient geophysical instruments.

The ROH possesses inherent weaknesses; including, a limited payload, fragile construction, and is difficult to operate and control. We examined alternative UAVs for use in GAUSS and concluded that suitable vehicles have been recently developed. The identified alternative UAV platforms are more advanced, complex, and expensive than ROHs.

The Geodimeter is the weakest subsystem of the GAUSS. The Geodimeter tracks the rover craft by using servo-mechanical motors to rotate the optical-sensor console as it follows the active-source, LED beacon. The response speed of the servo-mechanical motors is not adjustable. The maximum speed that can be followed without losing lock is, therefore, limited. Through our field

tests, we found that the Geodimeter provides better tracking results if it is stationed at least 25 m from the survey area.

We evaluated alternative positioning systems and believe recently-developed, differential global-positioning technology is suitable for GAUSS deployment for certain sites. We confirmed the retailer-stated accuracy of a few centimeters if the survey area is open (i.e., multipath is not a problem). Around buildings and trees, however, the accuracy rapidly deteriorated.

## **5.0 Conclusions**

During Phase I research, Geophex laid the foundation for an automated data-acquisition and processing system and designed applicable geophysical sensors. Performance of the subsystems was verified by stand-alone testing. Finally, we investigated the overall system design using hand-held, prototype instruments.

During Phase II, we refined the subsystems developed in Phase I and modified them for airborne applications. We evaluated the GAUSS under real conditions and demonstrated the ability to:

- maneuver the ROH with a custom fluxgate-magnetometer package and tracking unit,
- automatically acquire position, altimeter, and sensor data, and
- display the results of the survey in real-time.

The major accomplishments achieved during this research project include:

- Developing a robust survey-control software program that is capable of recording, processing, displaying, and storing geophysical and altimetry data, as well as spatial registry information in real-time,
- Designing and fabricating a custom-processing PCB for the Bartington fluxgate magnetic sensor,
- Developing algorithms to correct for the heading errors that are inherent to fluxgate magnetic sensors,
- Modifying our proprietary EM instrument for use in the GAUSS. Specific improvements include; 1) continuous data acquisition (sample rate of 2 Hz), 2) real-time data output (via a RS-232 port), 3) a single PCB instead of hand-wired protoboards, 4) reducing the power supplies from three battery packs to one, 5) minimizing the base-line drift and offset (through improved bucking), and 6) modifying the system algorithms to allow software-selectable waveforms (multifrequency capability),
- Integrating commercial positioning systems, RF modems, and survey vehicles into a fast, efficient data-acquisition system with error checking capabilities, and
- Acquiring sample data sets that demonstrate the successful completion of the stated objectives.

## **References**

Phase I Topical Report, March 1995, Submitted to the U.S. Department of Energy, Morgantown Energy Technology Center, Morgantown, West Virginia.



**Appendix A**  
ProxLink RF Modem Family Wireless RS-232 Connection

| <i>Specification</i>       | <i>ProxLink Models</i>                                                 |                 |
|----------------------------|------------------------------------------------------------------------|-----------------|
|                            | <b>PL</b>                                                              | <b>PL2</b>      |
| <b>Serial Interface</b>    |                                                                        |                 |
| Asynchronous               | ←-----1.2,2.4,4.8,9.6,19.2 Kbaud-----→                                 |                 |
| Data Format                | ←-----8N1,7E1,7O1-----→                                                |                 |
| In band flow control       | ←-----CTS, DSR, XON/XOFF-----→                                         |                 |
| Connector                  | ←-----9-pin female D connector-----→                                   |                 |
| <b>Radio*</b>              |                                                                        |                 |
| Power output               | 400mW(max.)                                                            | 500mW(max.)     |
| Data rate                  | 121 Kbps                                                               | 242 Kbps        |
| Independent channels       | 4                                                                      | 3               |
| Range (typical)**          | up to 1000 feet                                                        | up to 1000 feet |
| Frequency band             | 902-928 MHz                                                            |                 |
| <b>Power</b>               |                                                                        |                 |
| Source (regulated)         | ←-----9V-----→                                                         |                 |
| Transmit current           | ←-----350 mA @ 9V-----→                                                |                 |
| Typical current            | ←-----150mA-----→                                                      |                 |
| <b>Packaging</b>           |                                                                        |                 |
| Antenna                    | ←-----5/8 wave with 3 dB gain-----→                                    |                 |
| Package size (w/o antenna) | ←-----4.0" x 6.5" x 0.75"-----→                                        |                 |
| Weight (with antenna)      | ←-----12 ounces-----→                                                  |                 |
| <b>Environment</b>         |                                                                        |                 |
| Temp. (operating/storage)  | ←-----20° to 60° C/-50° to +85° C-----→                                |                 |
| Relative humidity          | ←-----20% to 90% (non-condensing)-----→                                |                 |
| <b>Software</b>            |                                                                        |                 |
| Operating Modes            |                                                                        |                 |
| Pass-through               | Transparent to application, off-line configuration                     |                 |
| Packetized                 | ProxLink accepts real-time configuration, message, and status commands |                 |
| Message format options     | Line length, delimiters, and input time-out                            |                 |
| Network Parameters         |                                                                        |                 |
| Channel options            | Radio channel and security subchannel (16 bits)                        |                 |
| Outgoing messages          | Point-to-point or broadcast                                            |                 |
| Incoming messages          | Point-to-point, broadcast, or all                                      |                 |
| Packetized Mode Features   | Standby mode                                                           |                 |

\* Proxim's ProxLink radio modules are certified under the FCC's (Part 15) spread spectrum regulations allowing for their unlicensed use in the United States.

\*\* Range will vary depending on a number of factors including the physical environment between ProxLink units.

## Appendix B

### Analysis of the Novatel RT-20 GPS System

Although Geophex's initial analysis of GPS systems indicated that commercial units were not suitable for GAUSS (Phase I Topical Report, March 1995), we re-evaluated commercial GPS systems in June, 1996, to determine if recent technological advancements had improved system performance and decreased weight requirements. We conducted field and laboratory tests of a DGPS manufactured by Novatel Communications Limited (model RT-20; Figure B-1). The objective our tests were to evaluate data format, update rate, accuracy, and sensor weight.

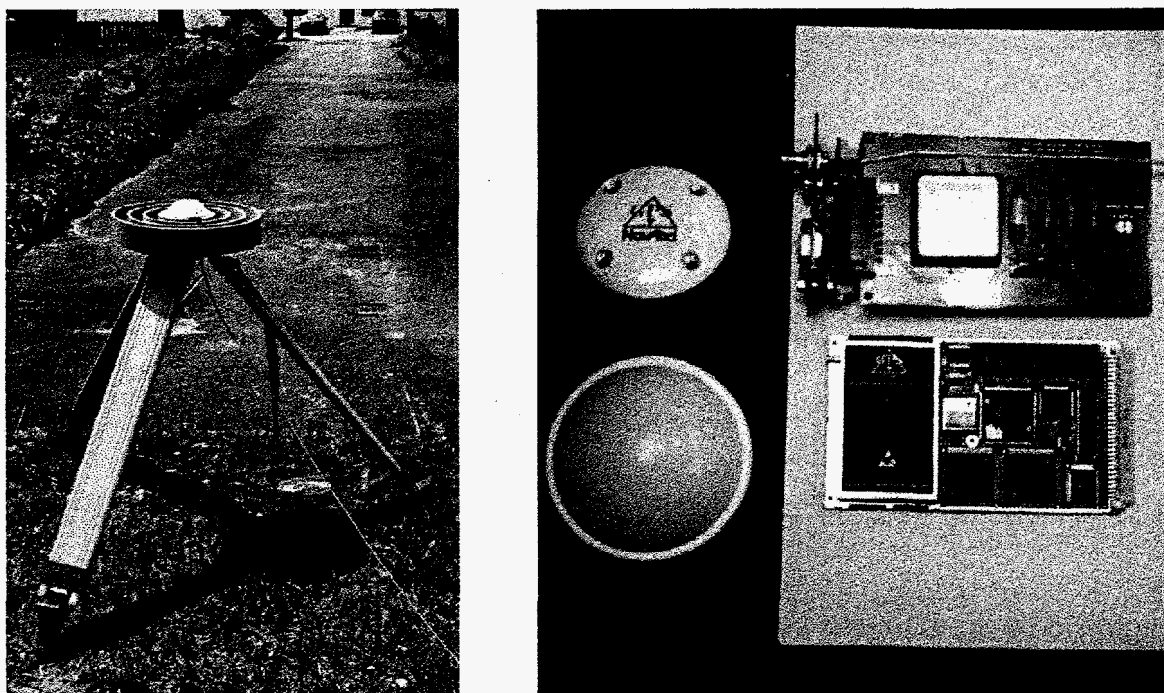


Figure B-1. Differential Global Positioning System; Novatel Communications Ltd., model RT-20. Left: base station; Right: antennae and OEM cards.

Our field tests indicated spatial resolution on the order of centimeters is attainable in open fields (clear sky view) but on the order of meters, or tens of meters, around buildings and trees due to multipath wave propagation. The weight of the rover antennae and associated electronic boards is suitable for UAV deployment (approximately 0.5 kg - this does not include the battery packs), and the data format is acceptable for the GAUSS Survey Control Software, given minor programming changes. The update rate is software changeable, with the fastest sampling occurring at 10 Hz.

If the survey area is suitable for DGPS (viz., multipath is not a problem), our tests indicate that this technology could be integrated into the GAUSS.

An advantage of GPS measurements is that line of site need not be maintained between the ROH and the base-station. For the GAUSS, however, this advantage is mitigated because the helicopter pilot must see the rover platform at all times.

C-1

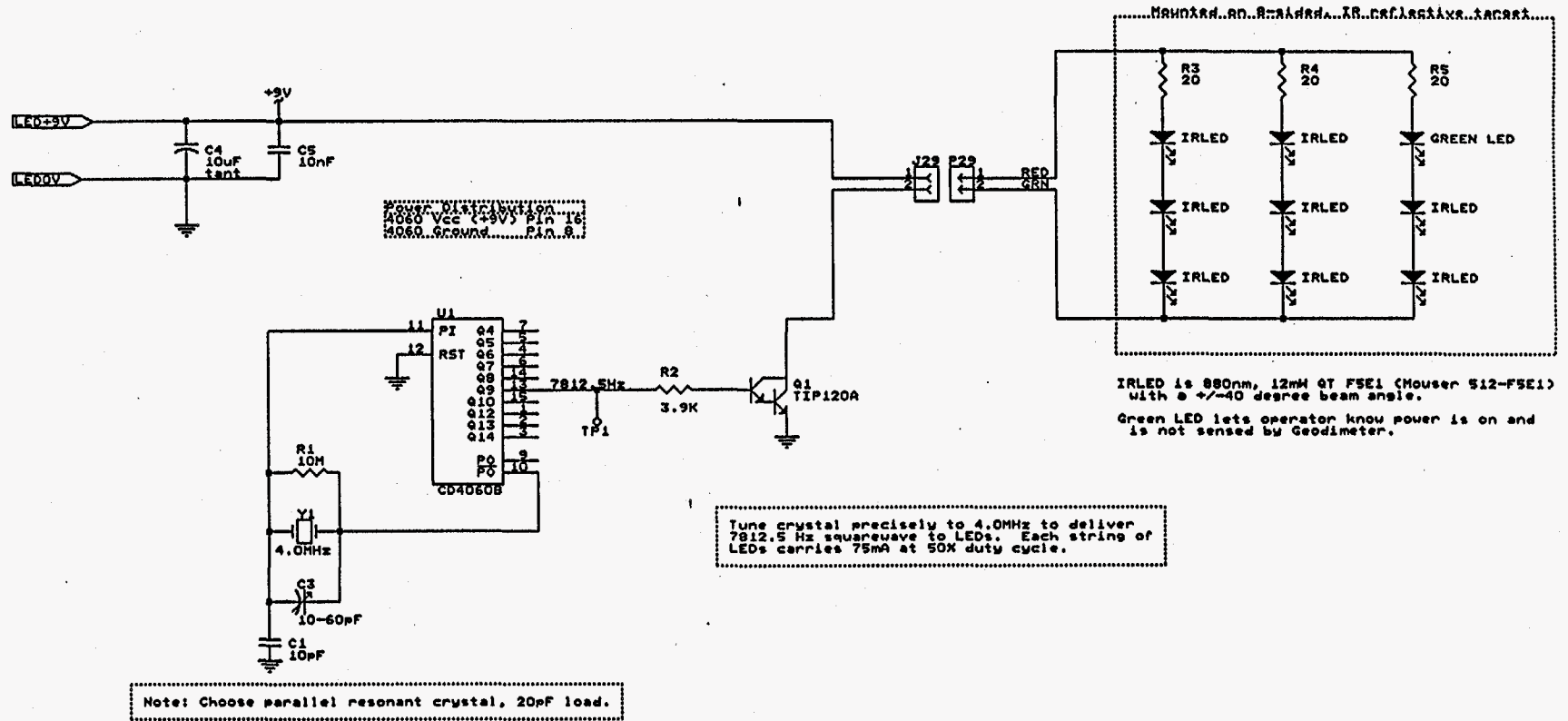


Figure C-1. Schematic of the omnidirectional LED beacon oscillator.

## Appendix D

### Cesium-vapor Magnetometer; the Geometrics model G-822A

The total field magnetometer is appropriate for low-altitude, airborne application because it provides stable output readings irrespective of orientation. Also, the total field instrument can detect ferrous objects at a range greater than a magnetic gradiometer. The two types of commercially-available, total-field sensors are the nuclear-precession and optical-pump magnetometers. The nuclear precession magnetometer is unsuited for the GAUSS due to its relatively slow update rate and substantial instrument weight.

Optical pump magnetometers, such as rubidium or cesium vapor instruments, provide highly accurate readings at suitable update rates ( $> 5$  per second) but, until recently, were too heavy for UAV deployment ( $\approx 20$  lb for a commercial cesium vapor unit). We tested a recently-developed, cesium-vapor magnetometer (Figure D-1) that was designed and manufactured by Geometrics for airborne applications.

The objectives of our analysis were to determine if the weight, power requirements, sampling rate, accuracy, and data format are acceptable for use in the GAUSS. Our results indicate that the sampling rate, data format, and sensor weight are acceptable and could be integrated into the GAUSS with minor modifications. The sensor requires 24-28 v, however, and the weight of the required battery pack is excessive. The sensor retails for eighteen thousand dollars.

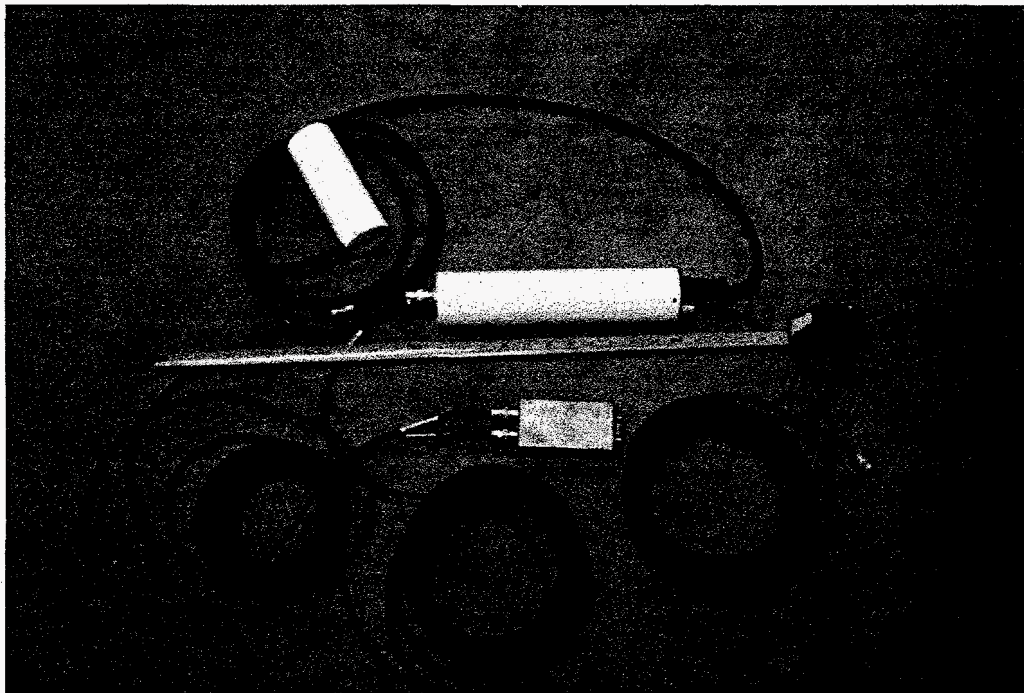


Figure D-1. Photograph of Geometrics G-822A cesium-vapor magnetometer. The unit consists of the sensor package (upper left), Lamar counter (middle), RS-232 output connector (bottom center), and cabling. Total weight is approximately 1.5 kg.

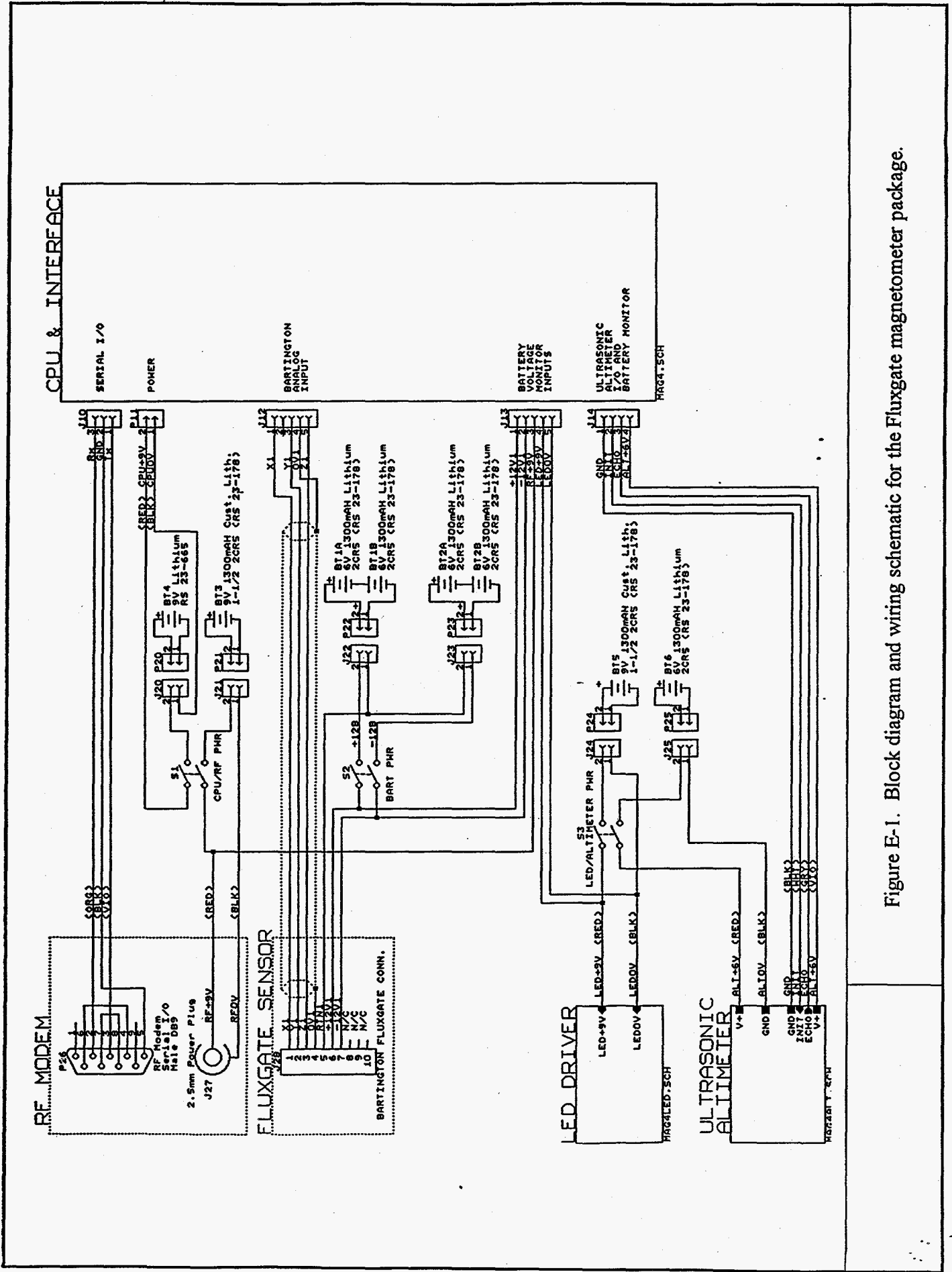


Figure E-1. Block diagram and wiring schematic for the Fluxgate magnetometer package.

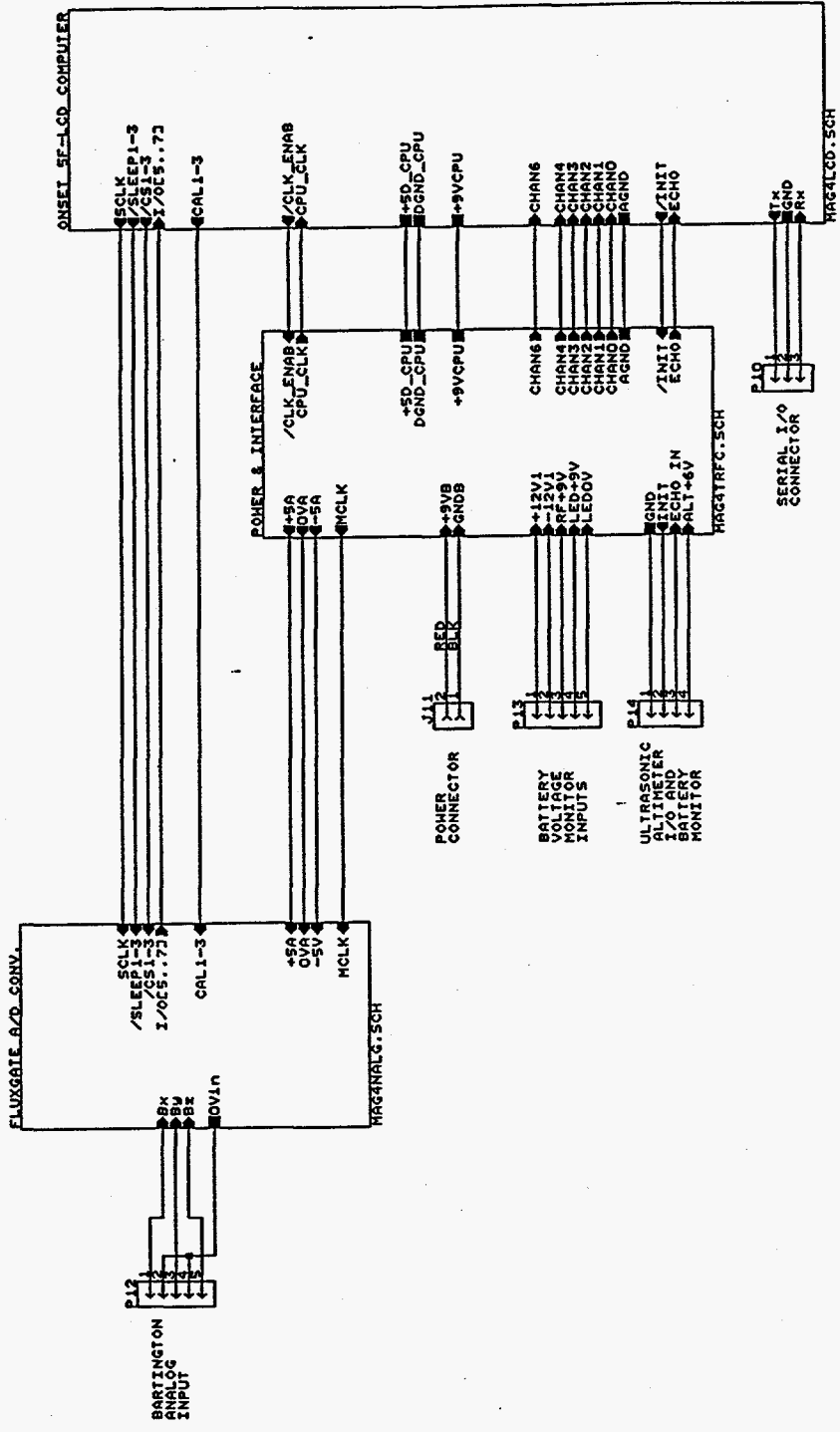


Figure E-2. Central processing unit (CPU) and interface diagram.

E-3

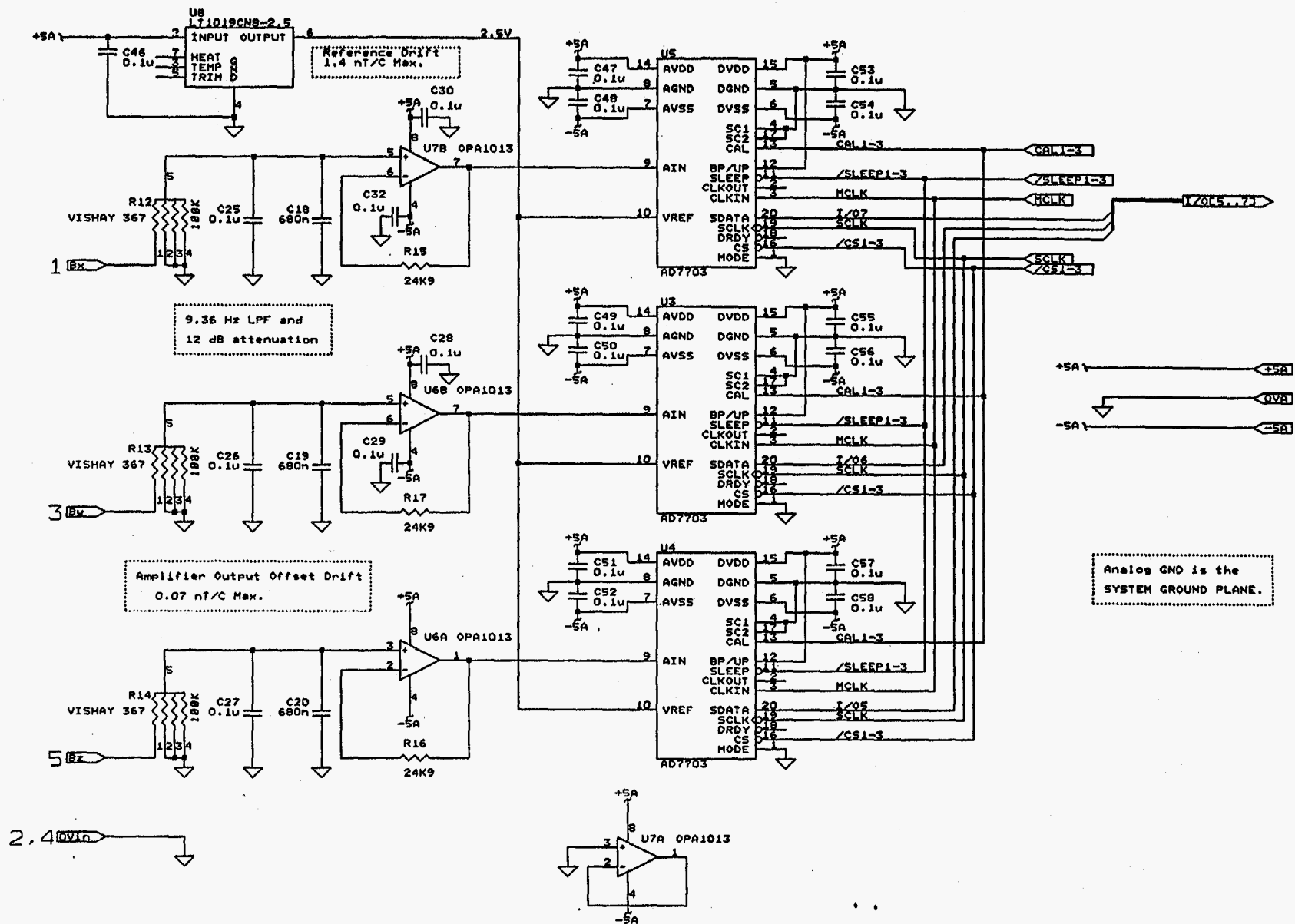
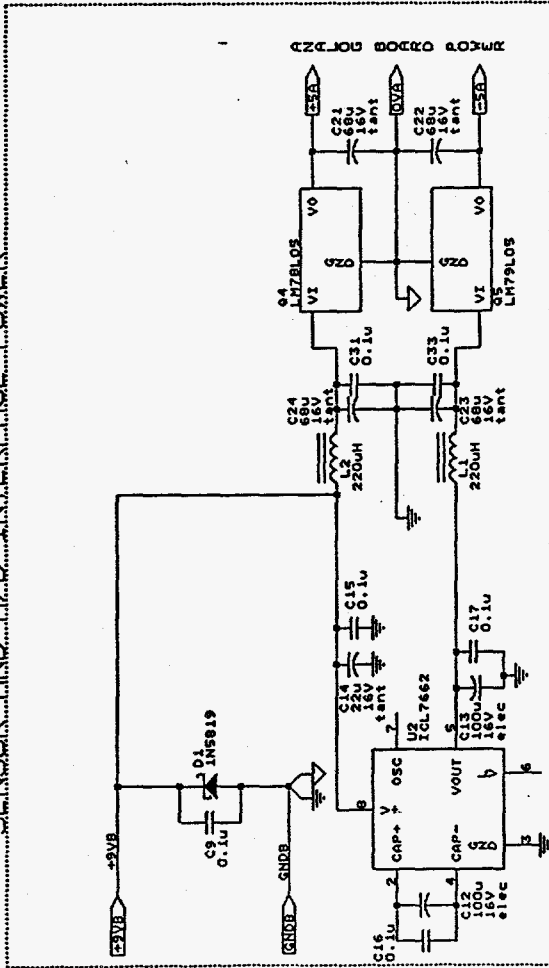
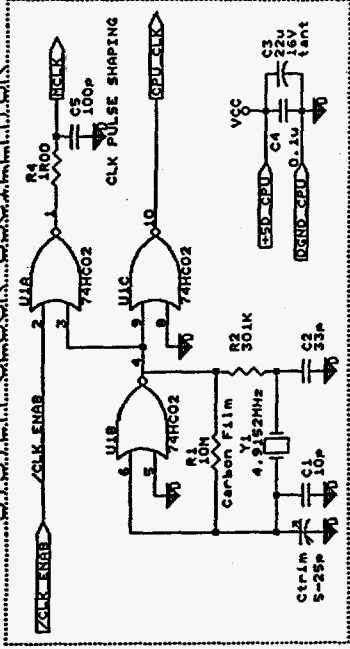


Figure E-3. Fluxgate A/D converter schematic.

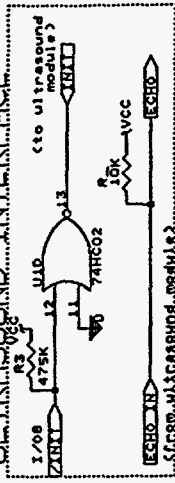
SENSOR AND A/D INTERFACE POWER



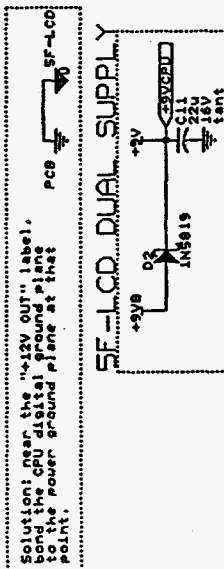
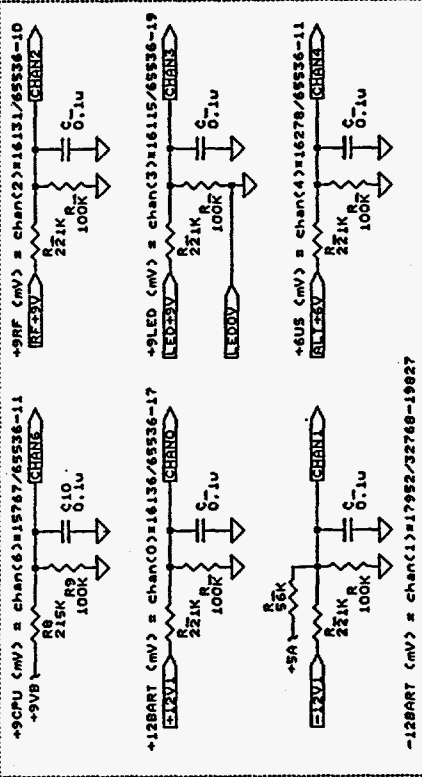
SYSTEM CLOCK OSCILLATOR



ULTRASOUND INTERFACE



BATTERY VOLTAGE MONITORS

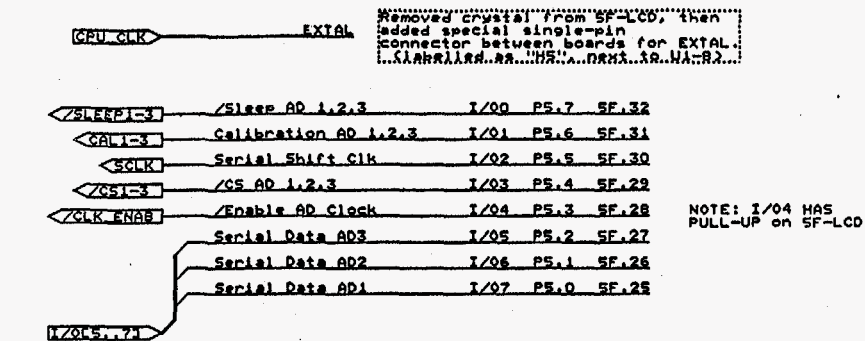


Solution: near the "+5V OUT" label, bond the CPU digital ground plane to the power ground plane at that point.

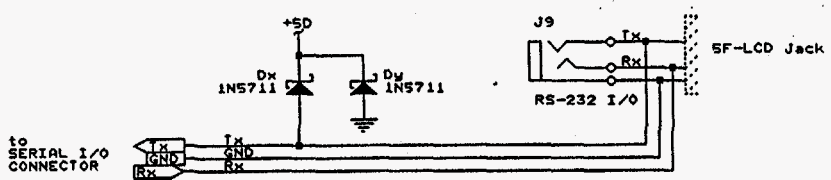
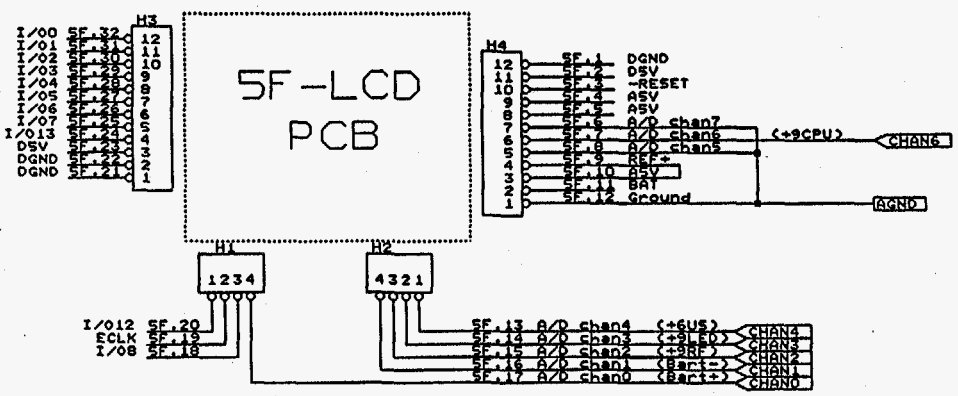
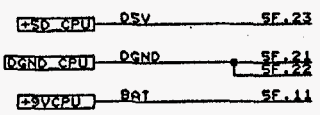
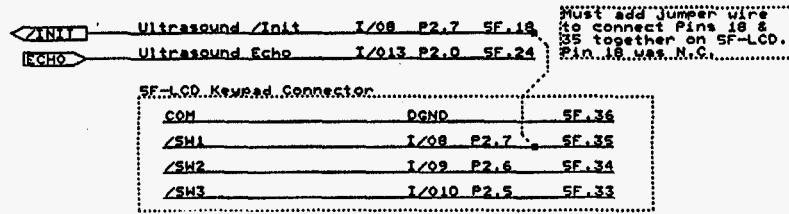
Note: all resistors in Metal Film unless otherwise noted.

Figure E-4. Power and interface schematic.



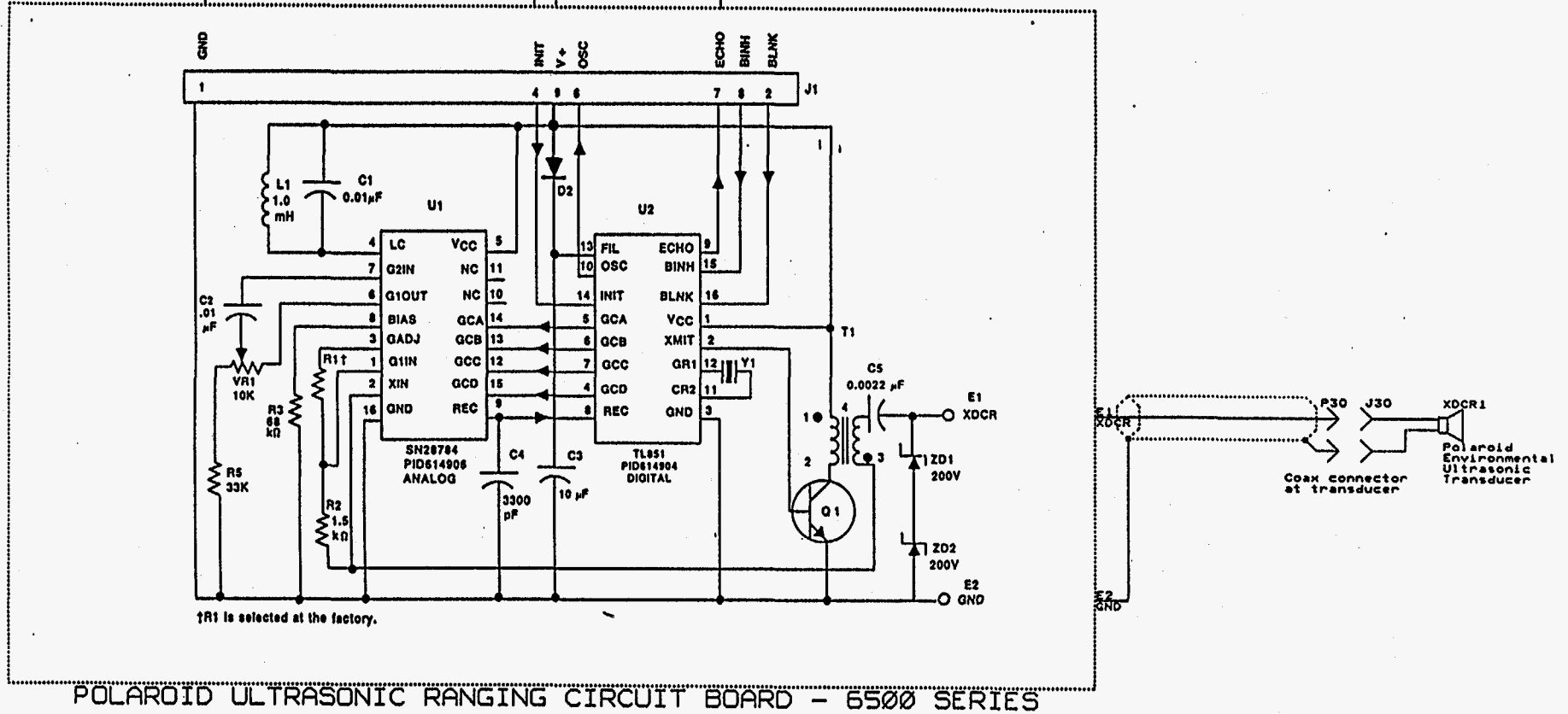
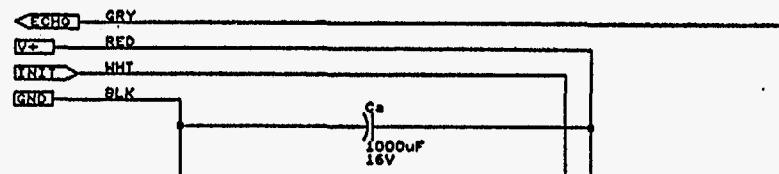


Note: Shows allocation of SF-LCD resources.



Note: SF.20 (I/O12) disabled on this board.

Figure E-5. Wiring diagram for the Onset 5F-LCD computer.



Note: Capacitor  $C_a$  added to buffer 2 amp surge currents pulled by ultrasonic driver during transmission phase.

Figure E-6. Wiring diagram of the Polaroid ultrasonic ranging circuit board.

## **Appendix F**

### **Description of the Geophex - Multifrequency Electromagnetic Sensor, GEM**

#### **Theoretical Basis for the GEM Sensor**

The basic principle of a frequency-domain electromagnetic (EM) system involves the measurement of change in mutual impedance between a pair of coils moving over the earth. A transmitter coil sets up a sinusoidally varying primary field that induces a system of currents within the earth below. This induced current, in turn, generates a secondary magnetic field generated by a dipole located at or above the surface of a layered earth. Some recent literature on EM sensor development is included in the references.

When the two coils are maximally coupled (i.e., in a mutually co-planar or coaxial configuration), the primary field at the receiver coil is very strong compared to the magnitude of the secondary induced field. It is desirable to remove this large field, mainly to reduce the dynamic range needed for the receiver preamplifier circuit. This can be accomplished by using a third coil, commonly termed a "bucking coil," that is placed between the transmitter and receiver coils.

The bucking coil is made so that its induced voltage from the primary field in the absence of the earth (i.e., in free space) is equal to that induced in the receiver coil. The bucking coil and receiver coil are wired in opposing (or bucking) polarity. By eliminating the primary field, the combined sensor unit thus produces a zero output in free space. When a conductive body (e.g., a steel UST) is present nearby, the sensor produces a differential output dependent only on the geometry and conductivity of the body.

The secondary field detected by the sensor is split into an in-phase and a quadrature (out-of phase) component. These are expressed in part-per-million (ppm) or part-per-thousand (ppt) against the primary field strength that would have been induced in an unbucked receiver coil. This complex quantity (real and imaginary) is called the mutual coupling ratio, and becomes the basis for subsequent data interpretation.

#### **General Description of the GEM Sensor**

GEM was designed to minimize temporal drift and insure calibration stability. The transmitter waveform is generated by means of a power H-bridge consisting of high-current Mosfet switching transistors. The H-bridge switches a DC voltage at a switching rate of about 72.9 kHz. The bridge, in turn, is digitally controlled by a pre-computed bitstream stored in battery-backed random-access memory (RAM). The output current waveform in the transmitter, thus, is digitally constructed by the binary series, through a well-established pulse-width modulation (PWM) technique. The binary series contains all the codes for a desired frequency constituent.

The receiver coil detects the earth response from below. The bucking coil is designed to cancel the strong primary field and also to produce the transmitter reference waveform. Both the signal and reference outputs from the receiver circuits are given to a Signal Processor unit that consists of an analog-to-digital (A/D) converter and a high-speed digital convolver.

Because we know precisely the transmitted waveform, the convolver (essentially a multiply and accumulate function, i.e., convolution) is instructed to pick only the transmitter frequency (or frequencies). This is accomplished by convolving the incoming signals with pre-programmed sine and cosine series (coinciding with the transmitter frequency) stored in a RAM look-up table. This detection scheme results in an extremely narrow bandwidth and, thus, enhances the signal-to-noise ratio (SNR) by an order of magnitude or more. The digitally processed data constitute the raw survey data.

Any metallic object other than the coils, such as the main console, generates a strong secondary field. This effect can be minimized by placing the console at a strategic location where the secondary field, as seen by the receiver, is at a minimum. This original technique was developed at Geophex for an airborne EM sensor for the US Navy. The console is packaged in an aluminum pod to attenuate high-frequency electromagnetic and electrostatic interference.

### **Hardware Descriptions**

The sensor is electronically partitioned into three sub-units:

- Control Processor Unit (CPU): runs the system and reduces the raw sampled data;
- Amplifier and A/D Unit: amplifies and filters the incoming signals and converts them to a digital format; and
- Transmitter Unit: generates timing signals and drives the transmitter coil using a power H-bridge.

All three sub-units are housed in a single console (a 2.5x4.25x10 inch rectangular box) located near the midpoint of the coil-support boom.

#### *Control Processor Unit*

The CPU contains a microprocessor that collects and processes the GEM data. The heart of the control processor is the Motorola 56001 CPU chip. One of its major features is an arithmetic unit containing a 24-bit parallel multiplier and two 56-bit accumulators. The advantage of this architecture is the ability to perform high-precision multiplications with little chance of overflow.

The other two parts of the control processor are the memory and the input/output (I/O) system. The memory used is a combination of low-power static RAM and EPROM. The 64k-byte EPROM is used to start up software stored in RAM. The RAM has a battery backup for power-off data retention and is organized into two banks of 64K-words. The memory is decoded using a programmable logic device. The RAM battery is independent of the main battery.

The I/O System is composed of various general-purpose I/O lines available from the CPU, one Read-Write port used for reading and writing to the console, and one serial port used for

transferring data and programs from the computer host. The general purpose port is used for controlling various functions of the receiver and transmitter and for monitoring the system status. The Read-Write Port is used for writing to the LCD display and for reading the positions of the panel buttons. The serial port is connected directly to an RS-232 driver chip.

#### *Amplifier and A/D Converter Unit*

This unit is designed as a dual-channel, instrumentation amplifier. Each channel incorporates passive band-pass filters having very high stability in their frequency response. The A/D converter has built-in, digital, low-pass filters with very sharp roll-off. These anti-aliasing filters eliminate the need for bulky, unstable, external anti-aliasing filter circuitry. The custom signal channel instrumentation amplifier has an input-referenced noise of less than  $3.4 \text{ nV}/\sqrt{\text{Hz}}$  over the sampled band-width and has a common-mode noise rejection (CMNR) ratio greater than 80 dB.

#### *Transmitter Unit*

The transmitter unit consists of a clock divider, EPROM addressed with a counter, and a monolithic power H-bridge. The clock divider is made using two ripple counters and a programmable logic device. This divider provides the timing signals needed for both the transmitter and the A/D on the amplifier. The EPROM is pre-programmed with waveforms for all the broadcast frequencies that can be selected, using one of the four address lines.

The waveforms are clocked from RAM to the H-bridge through a programmable logic device (PLD) that provides necessary interface logic. The H-bridge, with built-in temperature and current sensors, is a highly integrated device that provides circuitry to drive the internal FET's (field effect transistors) at an RMS (root-mean square) current of about 3 Amperes (6 amps peak). The bridge directly drives the transmitter coil that radiates the programmed waveforms.

#### **References**

The following references are provided for further reading.

- I.J. Won, 1983, A sweep-frequency electromagnetic exploration method, Chapter 2, in *Development of Geophysical Exploration Methods-4*, Editor; A. A. Fitch, Elsevier Applied Science Publishers, Ltd., London, p. 39-64.
- I.J. Won, 1985, Frequency-domain electromagnetic ice-sounding, in *Proceeding of the Arctic Oceanography Conference*, NSTL, Mississippi, p. 167-172.
- I.J. Won, 1986, High-resolution electromagnetic altimetry over the ocean, *IEEE Journal of Ocean Engineering*, v. OE-11, p. 327-332.
- I.J. Won and K. Smits, 1986, Application of the airborne electromagnetic method for the bathymetric charting in shallow oceans, in *Proceeding of Airborne Resistivity Workshop*, Canada Geological Survey, Paper 86-22, p. 99-106, Ottawa.

- I.J. Won and K. Smits, 1987, Airborne electromagnetic measurements of electrical conductivities of seawater and bottom sediments over shallow ocean, *Marine Geotechnology*, v. 7, p. 1-14.
- I.J. Won, 1990, Airborne electromagnetic bathymetry, in *Developments and Applications of Modern Airborne Electromagnetic Surveys*, Edited by D. V. Fitterman, US Geological Survey Bulletin 1925, p. 155-164.
- I.J. Won and K. Smits, 1991, Airborne electromagnetic bathymetry, geoexploration, special issue: *Developments in Geophysical Exploration Methods*, Editor, A. A. Fitch, v. 27, p. 297-319, Elsevier Applied Science Publishers, Ltd., London.
- Won, I. J., Keiswetter, D., Fields, G., and Sutton, L., 1996, GEM-2: A new multifrequency electromagnetic sensor: *Journal of Environmental and Engineering Geophysics*, v. 1, no. 2, p. 129-137.

## Appendix G

### Evaluation of a UAV developed by the University of Texas at Arlington

The University of Texas at Arlington's (UTA) aerial vehicle was designed to be rugged, simple, and easy to maintain while still having flexibility in its mission assignment (Figure G-1). The design includes a vertical take-off and landing aircraft, a rigid propeller, vehicle-stability augmentation system, navigation system, and autonomous control functions. The primary mission of the aircraft is to autonomously locate and recognize predefined targets, and map the location of each target.

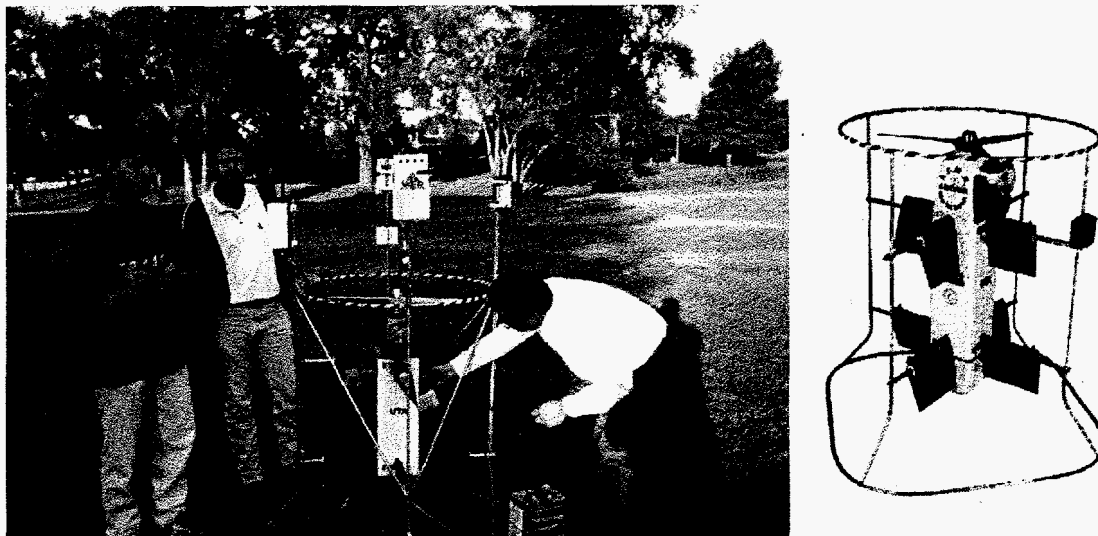


Figure G-1. UTA's autonomous unmanned vehicle, August 19, 1996.

Demonstrations of the data acquisition system (viz., GAUSS hardware and software mounted on UTA's UAV) were conducted on August 19-20, 1996, at two locales on the University of Texas at Arlington campus (Figure G-2).

A total of six flights were completed. Each flight was designed to test specific subsystems and to ensure that the aircraft, sensor, and acquisition hardware was functioning properly. Unfortunately, the UTA's UAV crashed during the second day of testing. The cause of the unprecedented crash is unknown, but may have been due to wind gusts, faulty gyros, the added weight of the geophysical hardware, or some combination of these factors.

We were able to record magnetic data during the preliminary test flights and display the results in real-time. Figure G-3 shows the magnitude of the magnetic field versus time as well as the aircraft's spatial position versus time for one of the test flights. Analysis of these data establishes the data reliability and allows us to identify spurious magnetic signatures. For example, the magnetometer output should remain relatively steady if the aircraft does not move, and should vary smoothly during the survey.

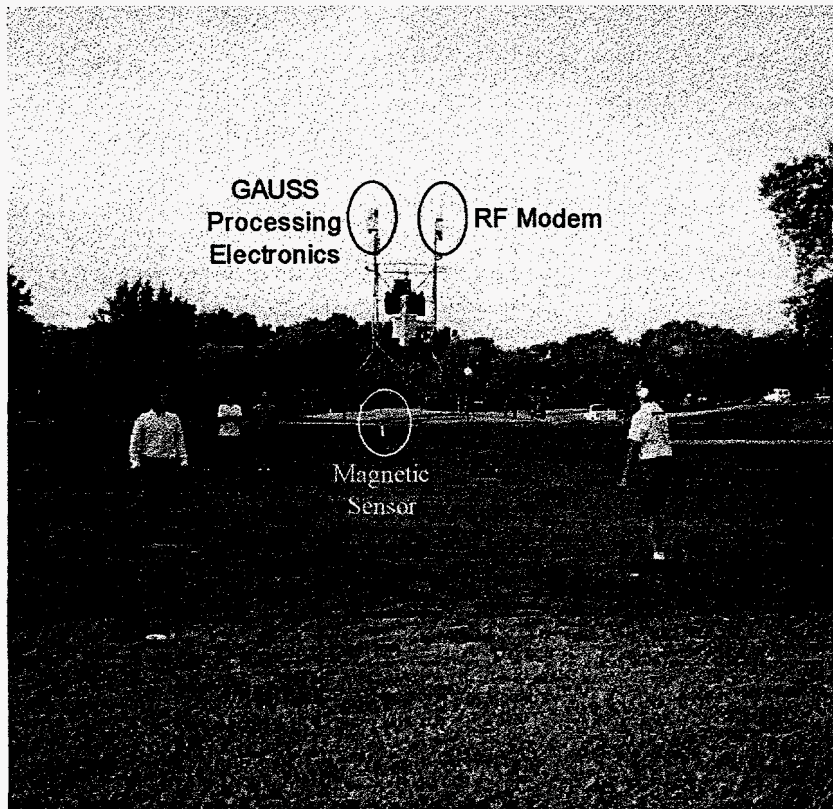


Figure G-2. UTA's aerial vehicle in flight, with GAUSS hardware mounted.

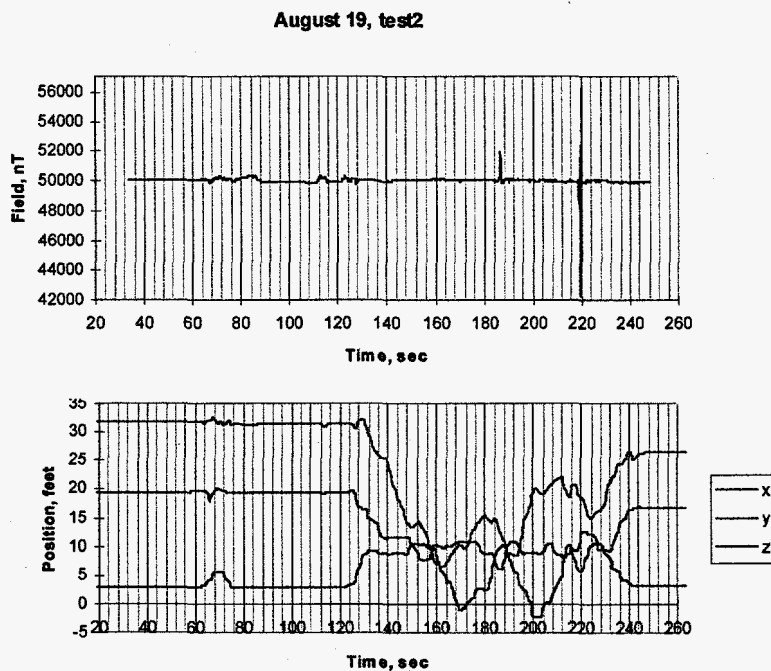


Figure G-3. Magnetic field and the position of the aerial vehicle versus time during the second test on August 19.



A cursory analysis of the data shown in Figure G-3 reveals two large, unexpected spikes in the measured magnetic field during data acquisition (times of 185 and 220 seconds). Although similar spikes were recorded during the other surveys, the source is not known at this time.

Because interpretation of the data in real-time is unreliable, due primarily to the spikes, we manually eliminated questionable data points. We combined the "cleaned-up" results of both surveys conducted on August 19 in one data file (Figure G-4). The anomalies located at coordinates (9.5, 12.5) and (9.5, 25.0) roughly coincide with the target locations.

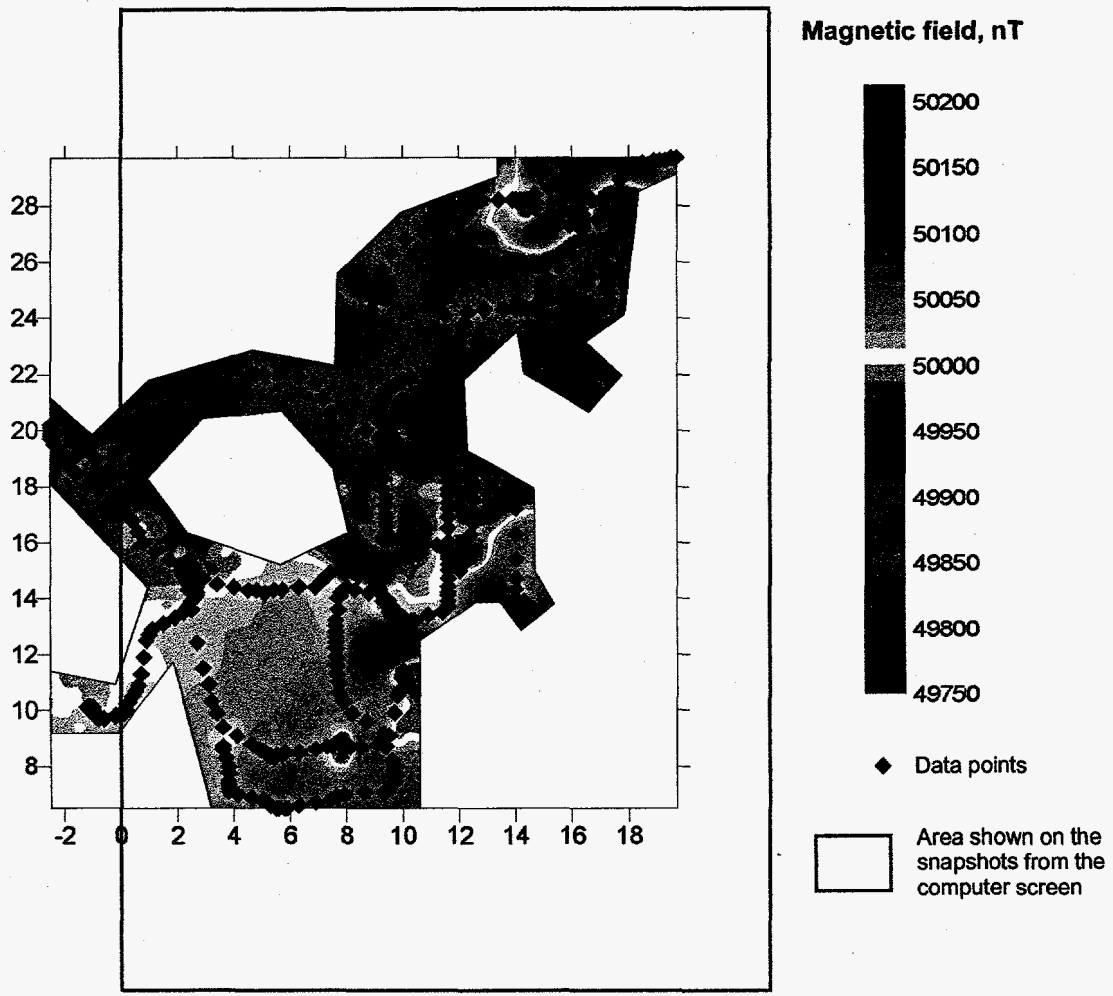


Figure G-4. Post-processed magnetic data from two surveys on August 19, 1996.

The joint effort was successful; we acquired and displayed magnetic data in real-time using the UTA UAV as the sensor platform. Although the project ended after the crash, we believe that the UTA's UAV can be redesigned for use as a successful geophysical-surveying platform. As with most small UAVs, the redesigned vehicle should have better control over horizontal motion, be more stable during the flight, be less subject to restrictions imposed by weather conditions, and be able to carry a 15-20 pound payload for 30-minute sorties.